
Site U1398¹

Expedition 340 Scientists²

Chapter contents

Background and objectives	1
Operations	1
Lithostratigraphy	3
Paleontology and biostratigraphy	4
Geochemistry	5
Physical properties	6
Paleomagnetism	7
References	9
Figures	10
Tables	24

Background and objectives

Integrated Ocean Drilling Program (IODP) Site U1398 (proposed Site CARI-09B; 14°16.70'N, 61°53.34'W; 2935 meters below sea level [mbsl]) is located west of Martinique (Fig. F1). The objective for this site was to characterize the sedimentation processes in the backarc Grenada Basin. We planned to drill through hemipelagic sediment and turbidites and retrieve a complete sedimentation record to ~264 meters below seafloor (mbsf). Site survey data showed that we could penetrate sedimentary reflectors indicative of the deposition of hemipelagic sediment and turbidites. With the recovered material we hope to identify the turbidites related primarily to debris avalanche deposition. One focus is to evaluate whether submarine debris avalanches can generate voluminous turbidites long after their emplacement and, if so, how far such turbidites can travel. We also expect to improve the reconstruction of the postcollapse eruptive activity of Pitons du Carbet (Boudon et al., 2007). This will provide better constraints on the transition of activity between the Pitons du Carbet and Montagne Pelée Volcanoes. Finally, we expect to sample turbidites with volcanic material coming from Dominica (e.g., Roseau tuff).

Operations

Transit to Site U1398

After a 46.0 nmi transit from Site U1397 in cruise mode, the vessel arrived at Site U1398. The vessel stabilized over Site U1398 at 0706 h on 24 March 2012. All times reported in this volume are given in ship local time, which was Universal Time Coordinated (UTC) – 4 h. The position reference was a combination of GPS signals and a single acoustic beacon. The positioning beacon was deployed at 0733 h on 24 March. At the end of operations at Site U1398, the beacon was sent an acoustic command to release. The beacon was retrieved at 1420 h on 28 March. The vessel was underway at 1430 h on 28 March to the next site.

Site U1398

Site U1398 consists of two holes (Table T1). The original plan called for two holes to be cored to ~264 mbsf. The first hole was successfully cored and was terminated at a total depth of 268.6 mbsf. The second hole was cored to 263.4 mbsf. Logging was planned for the triple combination (triple combo) and the Formation MicroScanner (FMS)-sonic tools strings, but hole problems forced the cancellation

¹Expedition 340 Scientists, 2013. Site U1398. *In* Le Friant, A., Ishizuka, O., Stroncik, N.A., and the Expedition 340 Scientists, *Proc. IODP, 340*: Tokyo (Integrated Ocean Drilling Program Management International, Inc.).

doi:10.2204/iodp.proc.340.108.2013

²Expedition 340 Scientists' addresses.



of the logging program during the attempt to run the first logging string. At the end of Hole U1398B, the drill string was pulled back so that the bit was at ~2800 meters below rig floor (mbrf), and the vessel began the 12 nmi transit to the next site in dynamic positioning mode. The advanced piston corer (APC) was deployed 35 times. The cored interval with the APC was 257.0 m with a recovery of 259.09 m of core (101%). The extended core barrel (XCB) was deployed 29 times. The cored interval with the XCB was 275.0 m with a recovery of only 42.75 m of core (16%). Overall recovery for Site U1398 was 57%. Total time spent on Site U1398 was 103.5 h.

Hole U1398A

The vessel arrived at the Site U1398 and was in position at 0706 h on 24 March 2012. Near the end of an uneventful pipe trip, the last 15 stands of pipe had to be measured and drifted. The top drive was then picked up, and the bit was spaced out to spud Hole U1398A. The initial corrected precision depth recorder (PDR) reading was 2944.1 mbrf. The bit was set at 2940 mbrf, and the hole was spudded at 1551 h on 24 March. The seafloor depth was calculated from the length of the first core (2.7 m) to be 2946.8 mbrf (2935.3 mbsl). On the attempt to recover Core 340-U1398A-3H, there was no penetration and no recovery. The XCB was installed for Cores 3X and 4X. After Core 4X, the APC was redeployed. Orientation was performed with the FlexIt tool up to and including Core 7H on all APC cores. Nonmagnetic core barrels were used with the APC for Cores 1H through 7H. After Core 7H, both the FlexIt orientation tool and the nonmagnetic barrels were removed from the coring assembly. Advanced piston corer temperature tool (APCT-3) measurements were taken on Cores 5H through 8H. APC coring continued through Core 13H. At 105.6 mbsf, the APC was removed and an XCB core barrel was dropped. XCB coring continued through Core 30X. Hole U1398A coring was terminated at 268.6 mbsf, after the depth objective was met. Eleven piston cores were taken over 86.3 m with a total recovery of 86.98 m of core. Nineteen XCB cores were taken over a 182.3 m interval. Only 28.11 m (15%) were recovered, and the hole was terminated at 268.6 mbsf. Overall core recovery for Hole U1398A was 43%. After the completion of XCB coring, the drill string was pulled back, the top drive was set back, and the bit cleared the seafloor at 0540 h on 26 March, ending Hole U1398A. Total time spent on Hole U1398A was 46.75 h.

Hole U1398B

After clearing the seafloor from Hole U1398A, the vessel was offset 20 m east, and Hole U1398B was

spudded at 0723 h on 26 March 2012. The seafloor depth was calculated from the length of the first core to be 2946.6 mbrf (2935.1 mbsl). Orientation was performed and nonmagnetic core barrels were used through Core 340-U1398B-11H. APCT-3 measurements were taken on Cores 4H, 8H, and 10H. Similar to Hole U1398A, most of the piston cores were partial strokes and the hole was advanced by recovery. After reaching refusal with the APC on Core 24H, the XCB was deployed and XCB coring continued to 263.4 mbsf. Coring was terminated after Core 34X. Twenty-four piston cores were taken over a 170.7 m interval with a total recovery of 172.11 m (101%) of core. Ten XCB cores were taken over a 92.7 m interval. Only 14.64 m (16%) were recovered, and the hole was terminated at 263.4 mbsf. Overall core recovery for Hole U1398B was 71%.

At the conclusion of coring, Hole U1398B was conditioned with a 25 bbl high-viscosity mud sweep and displaced with 133 bbl of 10.5 ppg mud and a go devil was pumped. The drill string was then pulled back to 3016 mbrf, the top drive was set back, knobies were added to the drill string, the bit was set at 84.91 mbsf, and the pipe was hung from the blocks. The Schlumberger wireline was then rigged up for logging, and the triple combo was deployed. While running in the hole with the triple combo tool string, the drill string became stuck. The tool string was then pulled back to the surface and rigged down. The top drive was picked up, rotation and circulation were reestablished, and the hole was worked vertically until all overpull was eliminated. At this point, because of the poor hole conditions, the nuclear sources were removed from the triple combo tool string. The triple combo was then redeployed but was unable to completely pass through the bottom-hole assembly (BHA), with only a couple of meters of the tool clearing the bit into open hole. After trying unsuccessfully to run the string down, the string was pulled back. At one point the logging tools became stuck, but they were eventually freed and the tools were then pulled back to the surface and rigged down. After laying out the triple combo tool string, we again had to pick up the top drive, and, using rotation and overpull, the drill string was worked free from the formation. The knobies were then laid out, the top drive was set back, and the drill string was pulled back to 2800 mbrf. The knobies were then installed, the drill floor was secured, and the acoustic beacon was recovered at 1420 h. At 1430 h on 28 March all activities at Site U1398 were completed, and the vessel then commenced the move to Site U1399 at 1.5 kt. Total time spent on Hole U1398B was 56.75 h.

Lithostratigraphy

Two holes were drilled at Site U1398: Hole U1398A was drilled to 260.5 mbsf, and Hole U1398B was drilled to 255 mbsf. A few preliminary correlations can be made between the holes, but there is considerable variability in the stratigraphy even though the holes are ~20 m apart. Correlation in the lower parts of the two holes is problematic because of the low recovery in Hole U1398A.

The lithostratigraphy of Site U1398 comprises seven units (A–G). The upper part of the core is dominated by volcanoclastic turbidites, whereas the lower portion is composed of various combinations of hemipelagic muds, volcanoclastic turbidites, and tephra layers. Each lithology is described in detail in “[Lithostratigraphy](#)” in the “[Site U1394](#)” chapter (Expedition 340 Scientists, 2013b).

Unit A

Depths: Hole U1398A = 0–40 mbsf, Hole U1398B = 0–41 mbsf

Unit A extends from 0 to 40 mbsf in Hole U1398A and from 0 to 41 mbsf in Hole U1398B. The top of Unit A comprises 70 cm of hemipelagic mud, with the uppermost 30 cm composed of oxidized brown hemipelagic mud with high water content. Below 70 cm, the main part of Unit A is composed of a series of thick (mainly massive) volcanoclastic turbidites. This series of turbidites is continuous in Hole U1398B and represents >95% of the unit, with hemipelagic mud representing <5% of this interval. Most of the sand layers are massive (i.e., not laminated), and some are normally graded. These layers generally contain pumice ($\leq 20\%$, with the exception of one turbidite that contains 40%). The upper turbidite is thick and massive and contains abundant pumice clasts (≤ 5 cm). The dominant component is represented by mineral crystals, which vary in proportion from 50% to 70%. The other components are massive lava clasts (<20%) and sparse bioclastic or detritic carbonates (10%). In Hole U1398A, pumiceous turbidites are observed in the uppermost 10 mbsf; lack of recovery between 10 and 32 mbsf prevents correlation with Hole U1398B. In general, turbidites in Hole U1398A are fewer in number and thinner than those in Hole U1398B. The upper few tens of centimeters of each core consistently contain an abnormal concentration of large pumice and lava clasts. This coarse deposit results from the collapse during coring of pumice and lava clasts from above and is a coring artifact.

Unit B

Depths: Hole U1398A: 40–57 mbsf, Hole U1398B = 41–58 mbsf

Unit B extends from 40 to 57 mbsf in Hole U1398A and from 41 to 58 mbsf in Hole U1398B. The upper part of Unit B consists of hemipelagic sediment interbedded with thin tephra layers; this finer grained part of Unit B is several meters thick in Holes U1398A and U1398B. The lower part of Unit B comprises a succession of massive, normally graded turbidite units, which can be as thick as 6 m. Turbidites occasionally display compositional laminations, grain-size layering, and parallel stratification in the upper part of each layer.

Unit C

Depths: Hole U1398A = 57–80 mbsf, Hole U1398B = 58–79 mbsf

Unit C extends from 57 to 80 mbsf in Hole U1398A and from 58 to 79 mbsf in Hole U1398B. Hemipelagic mud is interbedded with multiple thin tephra layers and thin turbidites in Unit C. Hemipelagic sediment makes up most of this unit. Debrites and a relatively thick turbidite (>2 m thick) also occur at 60 and ~70 mbsf, respectively, in Holes U1398A and U1398B. Turbidites generally contain pumice clasts, which are normally graded, and hemipelagic clay.

Unit D

Depths: Hole U1398A = 80–104 mbsf, Hole U1398B = 79–99 mbsf

Unit D extends from 80 to 104 mbsf in Hole U1398A and from 79 to 99 mbsf in Hole U1398B. This unit is composed of a succession of massive turbidite units that are a few meters thick. The turbidites, many of which display normal grading, are separated by hemipelagic sediment interbedded with thin tephra layers. The lower boundary of Unit D is the upper of two distinctive pink-colored ash layers.

Unit E

Depths: Hole U1398A = 104–115 mbsf, Hole U1398B = 99–115 mbsf

Unit E extends from 104 to 115 mbsf in Hole U1398A and from 99 to 115 mbsf in Hole U1398B. This unit is characterized by multiple tephra layers. It also contains a few turbidites that are generally <1 m thick and interbedded with hemipelagic sediment. In Hole U1398A, only the top 8 m of Unit E was recovered. Two pinkish, 1 cm thick, glassy ash layers are present in the upper half of Unit E. These ash layers are key markers for this site, which allow preliminary correlations between the two cores.

Unit F

Depths: Hole U1398A = 115–171 mbsf, Hole U1398B = 115–171 mbsf

Unit F extends from 115 to 171 mbsf. This unit is very well recovered in Hole U1398B but poorly recovered in Hole U1398A. The top of this unit is composed of a 3 m thick debrite followed by a succession of thick massive turbidites. Intercalation of multiple thin ash fall and small-scale turbidites occur below the massive turbidites. Deformed volcanoclastic sand layers are present at 127 and 133 mbsf in Hole U1398B, and they represent unusually strong deformation during coring.

Unit G

Depths: Hole U1398A = 171–260.5 mbsf (bottom of hole), Hole U1398B = 171–255 mbsf (bottom of hole)

Unit G extends from 171 to 260.5 mbsf in Hole U1398A and from 171 to 255 mbsf in Hole U1398B. In this unit, core recovery was poor in both Holes U1398A and U1398B. Unit G mostly comprises well-lithified, heavily bioturbated hemipelagic mudstones. This unit occasionally contains interbedded volcanoclastic sand layers that are potential tephra layers. A whitish to pinkish colored, 1 cm thick, glassy ash layer occurs at 232 mbsf in Hole U1398A and at 246 mbsf in Hole U1398B. This layer is probably a correlatable tephra for the two holes at this site.

Paleontology and biostratigraphy

Core catcher samples at Site U1398 contain calcareous nannofossils and planktonic and benthic foraminifers of varying abundances and at varying levels of preservation. Calcareous nannofossil and planktonic foraminiferal data both indicate ages within the late Pleistocene (Fig. F2), which suggests extremely high sedimentation rates (see “[Planktonic foraminifers](#)” for a discussion). Reworking of much older (early Pleistocene and late Pliocene) material is evident in several samples. Many of the core catcher samples at Site U1398 consist of very coarse grained material that contains numerous shallow-water benthic foraminifers and fragments of shell and coral. Well-preserved pteropod and heteropod shells, otoliths, and sponge spicules (Demospongiae) were also found in some hemipelagic samples.

Calcareous nannofossils

Nannofossils are moderately to well preserved throughout Site U1398, declining near the base. Throughout the entire sequence, species characteristic of the late Pleistocene were found. In both Holes U1398A and U1398B, *Emiliania huxleyi*, *Gephyrocapsa oceanica*, *Gephyrocapsa caribbeanica*, *Gephyrocapsa*

parallela, *Ceratolithus cristatus*, and *Ceratolithus telesmus* were observed. Thus, the entire sequence was placed in Zone CN15, which has a maximum age of 0.25 Ma (Okada and Bukry, 1980). The presence of late Miocene to early Pliocene species in Samples 340-U1398A-14X-CC, 20X-CC, 21X-CC, 24X-CC, 7H-CC, 9H-CC, 15H-CC, 26H-CC, 32X-CC, and 34X-CC suggests extensive reworking.

In Hole U1398A, *E. huxleyi* is absent in Samples 340-U1398A-21X-CC to 24X-CC, whereas in Hole U1398B it is only absent in Sample 340-U1398B-7H-CC. Consequently, these samples were placed within Zone CN14 (Okada and Bukry, 1980). Younger sediment (Zone CN15) was found below this sample; it should be considered reworked.

Planktonic foraminifers

Of the 30 core catcher samples from Hole U1398A, 29 were analyzed for planktonic foraminiferal content, along with 33 of the 34 core catcher samples from Hole U1398B. The remaining cores (Samples 340-U1398A-16X-CC and 340-U1398B-25H-CC) did not retrieve any material. Planktonic foraminifers were present in all samples, although some were found at very low abundances, possibly because of the high volume of volcanic material. In samples with abundant specimens, the assemblage of planktonic foraminifers was diverse but dominated by *Globigerinoides ruber* (white and pink), *Globigerinoides sacculifer*, and *Neogloboquadrina dutertrei* (dextral). Other abundant species include *Globorotalia truncatulinoides* and *Globorotalia tumida*. The fauna does not change significantly throughout Site U1398, and all species present are indicative of warm subtropical waters.

Several datum species were found in both Holes U1398A and U1398B; however, datum species were generally not found in samples with low planktonic foraminiferal abundance. *Globorotalia flexuosa* (0.07–0.40 Ma) and *Globigerinella calida* (bottom occurrence at 0.22 Ma) were found in low numbers in both holes. The presence of *G. calida* at the base of both Holes U1398A and U1398B dates the sediments to younger than 0.22 Ma, within the Pleistocene. The presence of *G. flexuosa* suggests a minimum age of 0.07 Ma; however, this estimate should be considered very weak because of the reworking of this sediment. The weakness of this estimate makes a definitive minimum age inappropriate, especially as specimens of *G. flexuosa* are largely, but not completely, confined to intervals with turbidites. Counter to the prediction based on species ranges, *G. calida* extends past the range of *G. flexuosa*. This suggests either error in the calibration of *G. calida*, or a regional difference in the occurrence of either *G. calida*

or *G. flexuosa*. A regional difference in *G. flexuosa* is perhaps the most likely explanation, as there is good agreement between the nannofossil biostratigraphy and the range of *G. calida*. However, paleomagnetic ages (see “[Paleomagnetism](#)”) do not agree with this biostratigraphic zonation.

The maximum biostratigraphic age suggests that sedimentation rates are much higher than originally anticipated. However, because of extensive reworking throughout this site and the small size of most *G. calida* specimens, further investigation will be needed to confirm this age. Several reworked coarse-grained samples from Holes U1398A and U1398B also contain datum species from the early Pleistocene and late Pliocene. Heavily abraded individuals of *Globorotalia tosaensis* (top occurrence [T] at 0.61 Ma) were found in Samples 340-U1398A-19X-CC and 23X-CC, whereas *Globorotalia exilis* (T 2.10 Ma) and *Globorotalia multicamerata* (T 2.99 Ma) were found in Samples 340-U1398B-7H-CC and 10H-CC, respectively. Because *G. exilis* and *G. multicamerata* unexpectedly co-occur here with *G. flexuosa* despite having non-concurrent ranges, they cannot indicate the true age of the sediment but instead might indicate an age for the sediment source of the mass flows between ~43 to ~58 mbsf and 70 to ~74 mbsf in Hole U1398B.

Benthic foraminifers

A total of 35 genera and 32 species were identified at Site U1398 in the >150 μm size fraction. Benthic foraminifers examined in Holes U1398A and U1398B varied in abundance, diversity, and preservation (poor to moderate). Twenty-five species are present in Hole U1398A and sixteen in Hole U1398B. Rotaliids have low diversity and are present in low abundances (1–10 specimens per sample) overall in Holes U1398A and U1398B. Several samples (19) contain noticeable amounts of *Amphistegina* (1–30 specimens per sample) and *Cibicides wuellerstorfi* (1–30 specimens per sample). *Amphistegina* sp. is common in reef environments (≤ 100 m depth), and their poor preservation is indicative of reworking consistent with the volcaniclastic sedimentation in the area. Buliminids were nearly absent except for Samples 340-U1398A-25X-CC, 28X-CC, 30X-CC, and 34X-CC, which contain overall low abundances (1–10 specimens per sample). Sample 340-U1398A-25X-CC is dominated by *Uvigerina peregrina* (110 specimens) and *U. peregrina* f. *parvula* (14 specimens). Similarly, miliolids are nearly absent in most samples, with the exception that *Pyrgo* is the dominant genus in Holes U1398A and U1398B and *Pyrgo murrhina* is the dominant species. Agglutinated foraminifers are extremely rare, with only two genera (*Bigenerina* and *Sigmoilopsis*) present. Benthic foraminiferal density is generally low at Site U1398, ranging between 1 and 60 foraminifers/g of

sediment, with the exception of Sample 340-U1398A-25X-CC, which has a density of 240 foraminifers/g of sediment.

At Site U1398, *Siphonodosaria cooperensis*, *Siphonodosaria sargrinensis*, and *Siphonodosaria pomuligera* are present in relatively low abundances (1–10 specimens per sample) in four samples. Single specimens of *S. cooperensis* are present in Samples 340-U1398A-25X-CC, 28X-CC, and 30X-CC, whereas *S. sargrinensis* and *S. pomuligera* are present in Sample 340-U1398B-34X-CC in low abundances (1–10 specimens per sample). The lack of dominant species in most samples makes it challenging to provide a robust paleodepth estimate. However, *C. wuellerstorfi* is common in middle–lower bathyal to abyssal settings and *P. murrhina* is common in middle to lower bathyal areas in the Grenada Basin (Galluzzo et al., 1990). Based on their very similar relative abundances and lack of other abyssal key taxa, a bathyal paleodepth is interpreted.

Geochemistry

Samples for headspace analyses were taken from 23 depths throughout Hole U1398A. Methane concentrations were only a few parts per million in the upper 180 mbsf and typical of those observed at previous sites. Below this depth, however, methane concentrations increased rapidly to a maximum value of 4700 ppm at 240 mbsf (Fig. F3). Despite these elevated methane levels, concentrations of the higher hydrocarbons remained close to detection limits, with between 0.4 and 1.4 ppm ethane and ethene measured in seven samples.

A total of 46 samples were taken for X-ray diffraction (XRD) and carbonate analysis. The only significant difference between the XRD patterns obtained at Site U1398 and those found at previous sites is that the deeper samples contain larger peaks for clay and quartz (Fig. F4).

Calcium carbonate concentrations are highly variable and are lower in intervals with higher proportions of volcanic material (Fig. F5; Table T2). Maximum concentrations are ~35 wt%, which partly reflects the greater proportion of terrestrial clay minerals and the absence of significant aragonite preservation.

Because of the coarse-grained nature of the sediment, it was not possible to take any pore water samples in the upper 60 mbsf at the site. In addition, one sample (from Section 340-U1398A-27X-1) contained a high proportion of coarse-grained material and was likely contaminated to some extent by circulating drill fluid (seawater). Hence, the uppermost pore water data come from Section 340-U1398A-9H-3 at a depth of 62.5 mbsf (Table T3). At this point pore water alkalinity

values are close to 10 mM and remain at this level to 150 mbsf. Alkalinity then gradually falls to 5.9 mM by 254 mbsf (Fig. F6A). We note the lower value for the sample at ~187 mbsf and that concentrations are also comparatively low for Cl and NH₄ (as compared to the surrounding fluids), and we suspect that this sample suffered from contamination during drilling. Ammonium concentrations increase steadily from 0.8 mM in the shallowest sample to ~1.6 mM in the deepest sample (Fig. F6B). Calcium concentrations decrease from 4.8 mM at 62.5 mbsf to 3.9 mM at 103 mbsf and then show an increase to 10.9 mM in the deepest sample (Fig. F6C). Magnesium concentrations show a gradual decrease from 51 mM in the shallowest sample to 44.4 mM at the base of the hole (Fig. F6D). Chloride concentrations show a consistent increase from close to the seawater value in the shallowest sample to 674 mM at 254 mbsf (Fig. F6E). Even the shallowest sample has ΣS concentrations that are less than half the seawater level, and ΣS falls to values near the detection limit by ~160 mbsf (Fig. F6F). Overall, data are consistent with diagenesis driven by oxidation of slightly higher levels of organic carbon than those seen in previous sites, coupled with a lesser contribution to the pore water profiles from alteration of volcanic material. The increase in chloride with depth may reflect hydration of clay minerals.

Physical properties

We used magnetic susceptibility to correlate Hole U1398B with Hole U1398A to 102 mbsf. High bulk densities and magnetic susceptibilities indicate the location of turbidites. Significant (>20%) variability in *P*-wave velocity exists over short (~5 m) depth intervals at both holes, with higher velocities often associated with more sand-rich sediment. Otherwise, there is no clear trend in *P*-wave velocity with depth. A linear fit to temperatures measured in the upper 74 m gives $57.4^\circ \pm 5.0^\circ\text{C}/\text{km}$.

Stratigraphic correlation between Holes U1398B and U1398A

We used magnetic susceptibility and natural gamma radiation (NGR) to correlate depths between Holes U1398B and U1398A (Figs. F7). We trimmed 10 cm off each end of the core sections in the NGR data and 5.1 cm in the magnetic susceptibility data to ensure minimization of edge effects during correlation. We then cross-referenced our correlations using NGR with magnetic susceptibility as a quality control measure. Hole U1398B was the reference hole for these correlations because it has the longest continuous record. Both holes have poor recovery at depths

below 110 mbsf, making it impossible to correlate below this depth. Correlation for the uppermost 7–10 m between holes is good, with clearly matching peaks in magnetic susceptibility throughout this range; however, between 10 and 50 mbsf major discrepancies exist between the two holes. It was especially difficult to find clear correlations between 30 and 50 mbsf. In general, correlations are strongest in the uppermost 10 m and between 60 and 102 mbsf. At all other depths, correlation is poor. Ultimately, we used magnetic susceptibility data to tie all points, with NGR as an additional guide. Below 102 mbsf, correlation is not feasible. Our correlation coefficient using magnetic susceptibility data is 0.46. This value is artificially low because of meter-scale gaps and several core breaks between data sets where no data exist (Analyseries software includes these zones to calculate correlation coefficient). The poorest correlation exists between 30 and 60 mbsf. In this depth range, both physical properties and stratigraphic data sets indicate different sediment depositional histories between sites. We therefore suggest that the poor correlation between 30 and 60 mbsf results from real geologic differences between holes. We were unable to make any correlations below 102 mbsf, and no correlations were made between 10 and 50 mbsf where there was limited recovery and significant stratigraphic differences. Where we did make correlations, depth shifts for Hole U1398B never exceed 2.5 m and rarely exceed 1 m. All picked correlation depth shifts are shown in Table T4.

Gamma ray attenuation density, magnetic susceptibility, and *P*-wave velocity

Sharp increases in magnetic susceptibility correlate with increases in sediment bulk density. These increases generally occur where coarse-grained sediments such as turbidites exist. *P*-wave velocities can be broadly grouped by sediment composition: volcanoclastic (1650–1850 m/s) and hemipelagic mud (1500–1600 m/s). Gamma ray attenuation (GRA) density and *P*-wave velocity commonly follow the behavior of magnetic susceptibility, with values decreasing upward within thick turbidites.

Shear strength

Undrained shear strength (S_u) measurements were not performed in the upper 40 and 60 m of Holes U1398A and U1398B, respectively, because of the presence of sandy and gravelly sediment. In Hole U1398A, S_u measurements were possible from 40 to 110 mbsf, and in Hole U1398B they were possible from 60 to 165 mbsf. The handheld penetrometer provided higher S_u measurements than those obtained with the automated vane shear (AVS) and the fall cone in

both holes. Although the set of S_u measurements is quite scattered in both holes, particularly those from the handheld penetrometer, we observe a general increase with increasing depth in both holes.

P-wave velocity

Discrete measurements of P -wave velocity measured on the x -axis (PW-X) match whole-core P -wave velocity measurements and are correlated with sediment composition. The lower range, consisting of hemipelagic sediment, is from 1500 to 1600 m/s, and the higher range, consisting of more sandy sediment, is from 1650 to 1890 m/s. P -wave velocities at this site show significant (>20%) scatter and no clear increase in P -wave velocity with depth.

Moisture and density

We collected 56 moisture and density (MAD) measurements (39 from Hole U1398A and 17 from Hole U1398B; Fig. F8). Despite the MAD data gap in Hole U1398A, no MAD samples were taken in Hole U1398B between 12 and 30 mbsf because those cores contained highly disturbed sand. The porosity of 42 hemipelagic samples ranges between 60% and 75%, with three samples having lower porosities between 50% and 60%. Volcanic sand samples have porosities between 39% and 67%. Calculated porosity values in high-permeability volcanoclastic sediment may be inaccurate. Values may be too low because the samples drain water during sampling, including on the core deck, during splitting, and when the MAD sample is extracted from the split core. Alternatively, where core recovery, handling, or splitting processes reorganize sand grains, sediment may become undercompacted and yield anomalously high porosities. Bulk density of hemipelagic sediment has a narrow range between 1.46 and 1.77 g/cm³. Volcanoclastic sediment has bulk densities as high as 2.2 g/cm³, and three samples have values as low as 1.52 g/cm³. Grain density for hemipelagic sediment ranges between 2.6 and 2.8 g/cm³ (with one exception: 2.3 g/cm³). Volcanoclastic sediment has similar grain density.

Thermal conductivity

Thermal conductivity was measured at 51 depths. The mean value was 1.034 W/(m·K) with a standard deviation of 0.086 W/(m·K) and a standard error on the mean of 0.012 W/(m·K).

Downhole temperature measurements

Temperature was measured with the APCT-3 at the bottom of Cores 340-U1398A-6H and 8H (45.6 and 60.4 mbsf, respectively) and Cores 340-U1398B-4H, 8H, and 10H (26.5, 58.1, and 73.8 mbsf, respectively).

Measurements attempted for Core 340-U1398B-7H were compromised by fluid circulation. Attempted measurements at the bottom of Core 340-U1398B-3H were not successful because of instrument failure. Downhole temperature was monitored for 674, 670, 673, 208, and 655 s, respectively. Temperature was calculated from these time series of temperature measurements using TP-Fit (see APCT-3 user manual on the Cumulus/Techdoc database at iodp.tamu.edu/tasapps/). We assume a thermal conductivity (k) of 1.0 W/(m·K) and $\rho C = 3.7 \times 10^6$ J/m³K. To calculate uncertainty, we assume k ranges from 0.9 to 1.1 W/(m·K) and ρC is between 3.2×10^6 and 4.0×10^6 J/m³K. At the base of Cores 340-U1398A-6H and 8H we obtained temperatures of $7.55^\circ \pm 0.05^\circ\text{C}$ and $7.97^\circ \pm 0.05^\circ\text{C}$, respectively. At the base of Cores 340-U1398B-4H, 8H, and 10H we obtained temperatures of $6.06^\circ \pm 0.02^\circ\text{C}$, $7.65^\circ \pm 0.07^\circ\text{C}$, and $8.41^\circ \pm 0.02^\circ\text{C}$, respectively. Uncertainties are greater than the error on the best-fit solution and the probe's measurement accuracy and are dominated by uncertainties in the thermal properties of the sediment. The temperature of ocean water at the seafloor is 4.24°C .

A best-fit linear relationship between depth and our six temperature measurements gives a temperature gradient of $57.4^\circ \pm 5.1^\circ\text{C}/\text{km}$ (Fig. F9). Using measured thermal conductivity, the implied heat flow is 59 ± 5 mW/m². This estimate does not need a correction for bathymetry, and sedimentation lowers the measured near-surface heat flow by as much as 4% (Manga et al., 2012). Of all the sites, this is the only one where a quadratic fit to the data (rather than a linear fit) produces a quadratic term that is statistically significant; however, modeling of this data indicates that a linear fit is still favored (Manga et al., 2012). As a consequence, we cannot conclude that the temperature measurements indicate fluid advection.

Paleomagnetism

Cores 340-U1398A-1H, 2H, 5H through 7H, and 340-U1398B-1H through 11H were recovered using the APC and nonmagnetic core barrels. Cores 340-U1398A-8H through 13H and 340-U1398B-12H through 24H were recovered using the APC and standard steel core barrels. The FlexIt core orientation tool was used on all cores recovered with the APC and nonmagnetic barrels; thus, between 0 and 51 mbsf in Hole U1398A and between 0 and 83 mbsf in Hole U1398B, declination can be corrected to true north. Where FlexIt tool data were not available, declination was guided by the discrete inclination (orange data, Figs. F10, F11; see "Paleomagnetism" in the "Methods" chapter [Expedition 340 Scientists, 2013a]). Expected inclination for the site is 27°

during normal polarity and -27° during reversed polarity, assuming a geocentric axial dipole (GAD). Archive halves of cores from Holes U1398A and U1398B were measured on the three-axis superconducting rock magnetometer (SRM) at 2.5 cm intervals (Table T5). NRM was measured before (NRM₀) and after stepwise alternating field demagnetization at 20 mT (NRM₂₀). Thirty-nine discrete samples were collected from the center of the working half of the core to compare to the SRM data (see “**Paleomagnetism**” in the “Methods” chapter [Expedition 340 Scientists, 2013a]). Three Hole U1398B samples (from 43, 186.7, and 246.2 mbsf) were stepwise demagnetized to 100 mT and also given an anhysteretic remanent magnetization (ARM) and an isothermal remanent magnetization (IRM) in fields of 20, 100, 300, and 1000 mT to assess their magnetic mineral composition (see “**Paleomagnetism**” in the “Methods” chapter [Expedition 340 Scientists, 2013a]).

Sediment recovered from Site U1398 was heterogeneous in composition and varied between layers of hemipelagic sediment and volcanoclastic tephra and turbidites (see “**Lithostratigraphy**”). Using the detailed core description logs, we only interpreted data measured on identifiable hemipelagic layers, as these appear the least disturbed and are more likely to provide information on the behavior of the geomagnetic field.

Results

NRM₀ (red) and NRM₂₀ (blue) intensities are shown for Holes U1398A and U1398B in Figures F10 and F11. NRM₀ intensity is relatively high at ~ 0.5 – 1 m/A. NRM₂₀ is $<10\%$ of NRM₀. This percentage reflects both the low coercivity of the sediment and the susceptibility of the material to acquire a strong drill string overprint. This overprint is typically removed by 20 mT when using nonmagnetic barrels, though significant overprinting and remagnetization of sediment when standard steel barrels are used is a persistent feature of Expedition 340 cores.

Hemipelagic sediment is highly discontinuous at Site U1398, punctuated by the significant thicknesses of turbidites, and comparison between the two holes is not as straightforward as for other sites (see “**Lithostratigraphy**” and “**Physical properties**”). Rifling of the core barrel is evident by scattered declination values in all cores recovered with the XCB; thus, inclination is the only indicator of polarity below 108 mbsf in Hole U1398A and 171 mbsf in Hole U1398B.

Between 0 and ~ 170 mbsf in Holes U1398A and U1398B, all SRM and discrete inclination data show scattered but positive inclination, clustering around

the expected GAD inclination. Similarly, declination shows little variation, suggesting that all sediment above 170 mbsf was deposited under normal polarity conditions and within the Brunhes Chron (<780 ka). These ages agree with biostratigraphic datums from planktonic foraminifers and nannofossils, suggesting the bases of Holes U1398A and Hole U1398B are no older than 250 ka.

Below 170 mbsf the inclination record from hemipelagic sediment becomes increasingly discontinuous because of poor recovery. However, negative inclination is a persisting feature evident in both SRM data and discrete samples indicating material older than 780 ka. This is in conflict with biostratigraphic ages (see “**Paleontology and biostratigraphy**”); thus, additional rock magnetic tests were performed to assess the nature of the remanence carrying material. Three discrete samples, two from horizons with negative inclination and one from the upper part of the record with positive inclination, were demagnetized and given an ARM and IRMs (Fig. F12). NRM is $\sim 4\times$ weaker and more resistant to demagnetization in the deeper samples, but inclination appears strong and stable in all three samples, suggesting the negative inclination is not an overprinted and/or a viscous artifact. All three samples show $>85\%$ acquisition of the 1000 mT IRM (SIRM) in a field of 300 mT, suggesting ferrimagnetic minerals (probably magnetite and maghemite phases) are the main remanence carriers throughout the core. Magnetic grain size, estimated by ARM/SIRM, shows no significant difference between samples, suggesting that magnetic grain size and mineralogy do not vary greatly throughout the core.

Consistently negative inclination in the lower parts of Holes U1398A and U1398B span over ~ 80 m with a single period of positive inclination at ~ 220 mbsf. This sediment was exclusively recovered with the XCB, and the deepest sediment is from a mostly intact semilithified mudstone. Inclinations are generally shallower than would be expected by a GAD model, and without declination to reinforce the shallow inclination values, definitive interpretation of polarity is difficult. Some sections of core do show evidence for postdepositional deformation; however, this cannot account for all the negative inclination intervals (see “**Lithostratigraphy**”). If indeed these consistently negative values show true geomagnetic behavior, it would suggest that sediment deeper than ~ 170 mbsf was deposited at a time that experienced reversed polarity and is older than 780 ka. However, this is inconsistent with relatively young biostratigraphic ages, and further detailed measurement is needed to provide constraint on the paleomagnetic data below ~ 170 mbsf at Site U1398.

References

- Boudon, G., Le Friant, A., Komorowski, J.-C., Deplus, C., and Semet, M.P., 2007. Volcano flank instability in the Lesser Antilles arc: diversity of scale, processes, and temporal recurrence. *J. Geophys. Res., [Solid Earth]*, 112:B08205. doi:10.1029/2006JB004674
- Expedition 340 Scientists, 2013a. Methods. In Le Friant, A., Ishizuka, O., Stroncik, N.A., and the Expedition 340 Scientists, *Proc. IODP, 340*: Tokyo (Integrated Ocean Drilling Program Management International, Inc.). doi:10.2204/iodp.proc.340.102.2013
- Expedition 340 Scientists, 2013b. Site U1394. In Le Friant, A., Ishizuka, O., Stroncik, N.A., and the Expedition 340 Scientists, *Proc. IODP, 340*: Tokyo (Integrated Ocean Drilling Program Management International, Inc.). doi:10.2204/iodp.proc.340.104.2013
- Galluzzo, J.J., Sen Gupta, B.K., and Pujos, M., 1990. Holocene deep-sea foraminifera of the Grenada Basin. *J. Foraminiferal Res.*, 20(3):195–211. doi:10.2113/gsjfr.20.3.195
- Manga, M., Hornbach, M.J., Le Friant, A., Ishizuka, O., Stroncik, N., Adachi, T., Aljahdali, M., Boudon, G., Breitung, C., Fraass, A., Fujinawa, A., Hatfield, R., Jutzeler, M., Kataoka, K., Lafuerza, S., Maeno, F., Martinez-Colon, M., McCanta, M., Morgan, S., Palmer, M.R., Saito, T., Slagle, A., Stinton, A.J., Subramanyam, K.S.V., Tamura, Y., Talling, P.J., Villemant, B., Wall-Palmer, D., and Wang, F., 2012. Heat flow in the Lesser Antilles island arc and adjacent backarc Grenada Basin. *Geochem., Geophys., Geosyst.*, 13:Q08007. doi:10.1029/2012GC004260
- Okada, H., and Bukry, D., 1980. Supplementary modification and introduction of code numbers to the low-latitude coccolith biostratigraphic zonation (Bukry, 1973; 1975). *Mar. Micropaleontol.*, 5:321–325. doi:10.1016/0377-8398(80)90016-X

Publication: 17 August 2013
MS 340-108

Figure F1. Site U1398 maps. A. Shaded image of topography-bathymetry and chaotic deposits (interpreted as debris avalanche deposits). (Continued on next page.)

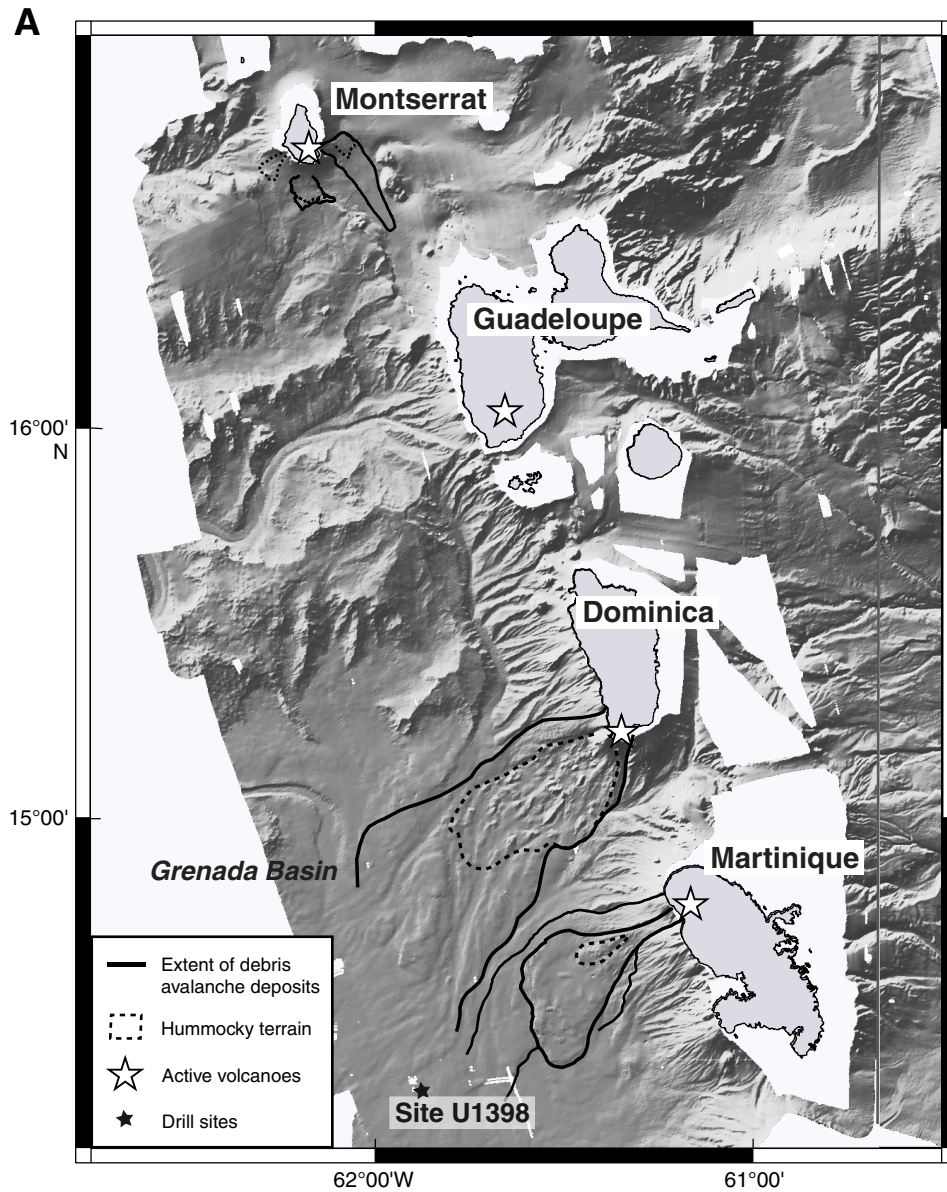


Figure F2. Integrated nannofossil and planktonic foraminiferal biozonation, Site U1398.

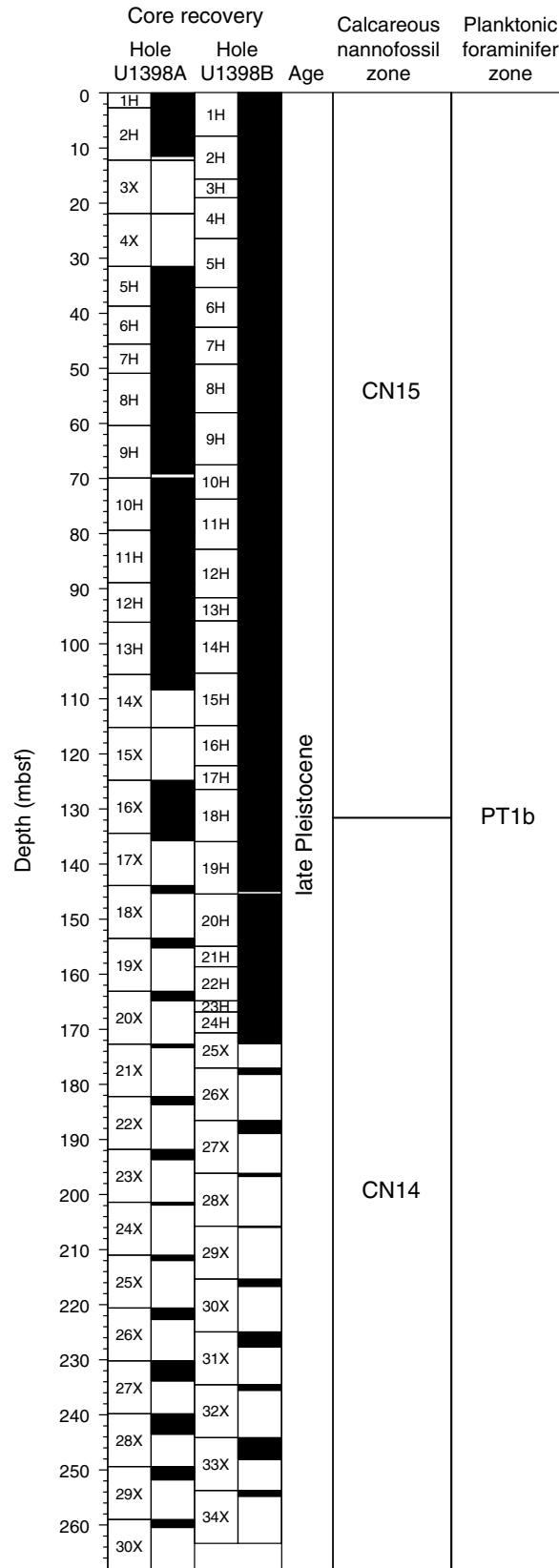


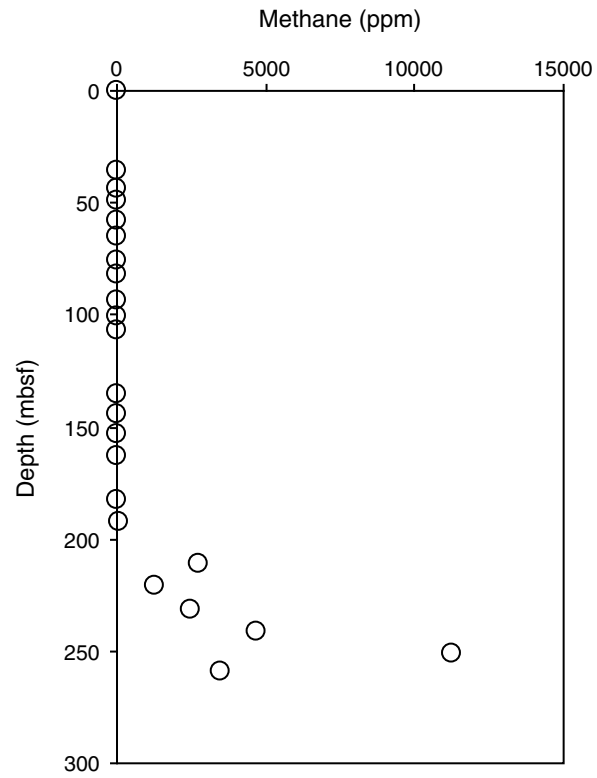
Figure F3. Headspace methane concentrations, Site U1398.



Figure F4. XRD pattern of Sample 340-U1398A-30X, 41–42 cm.

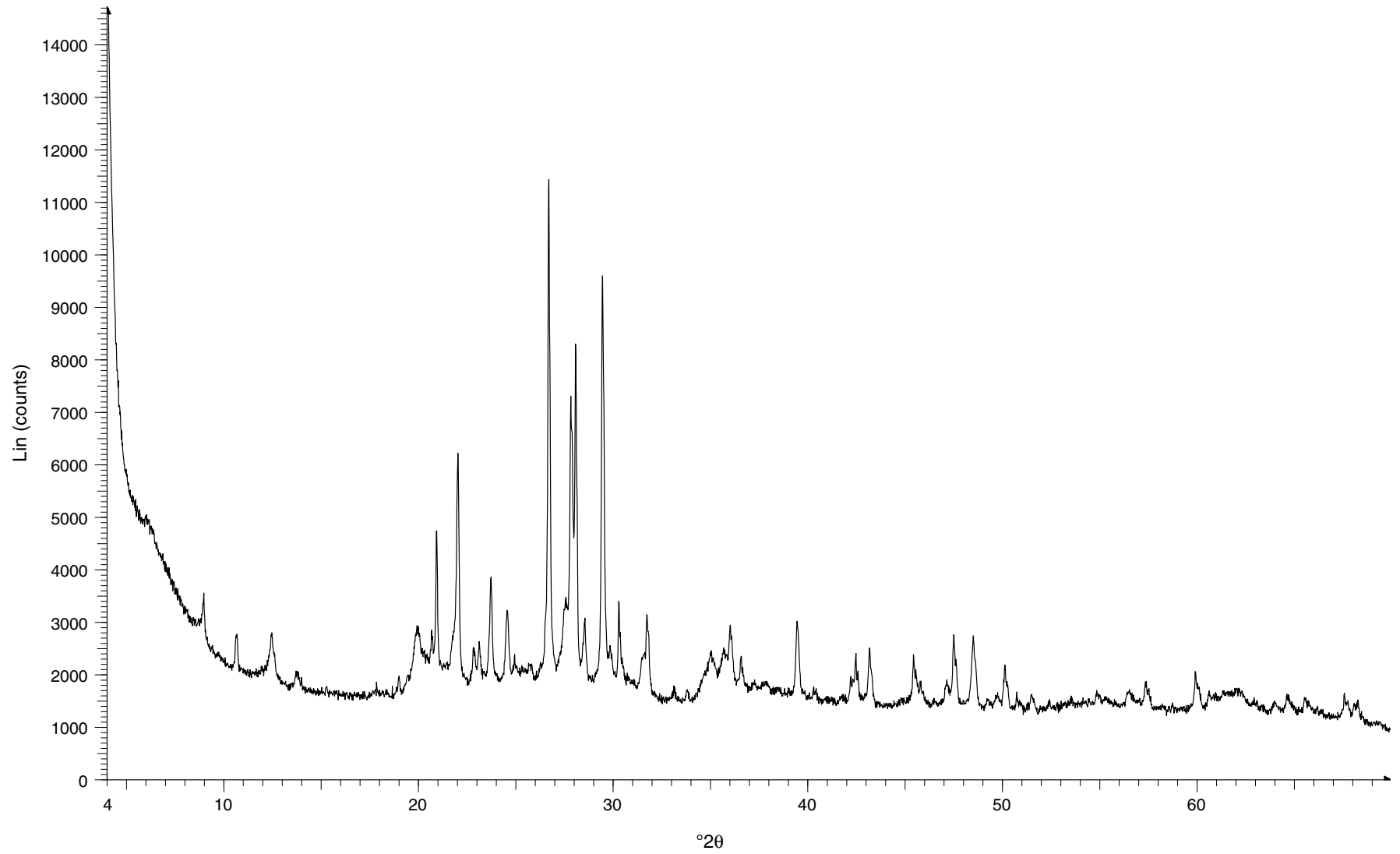


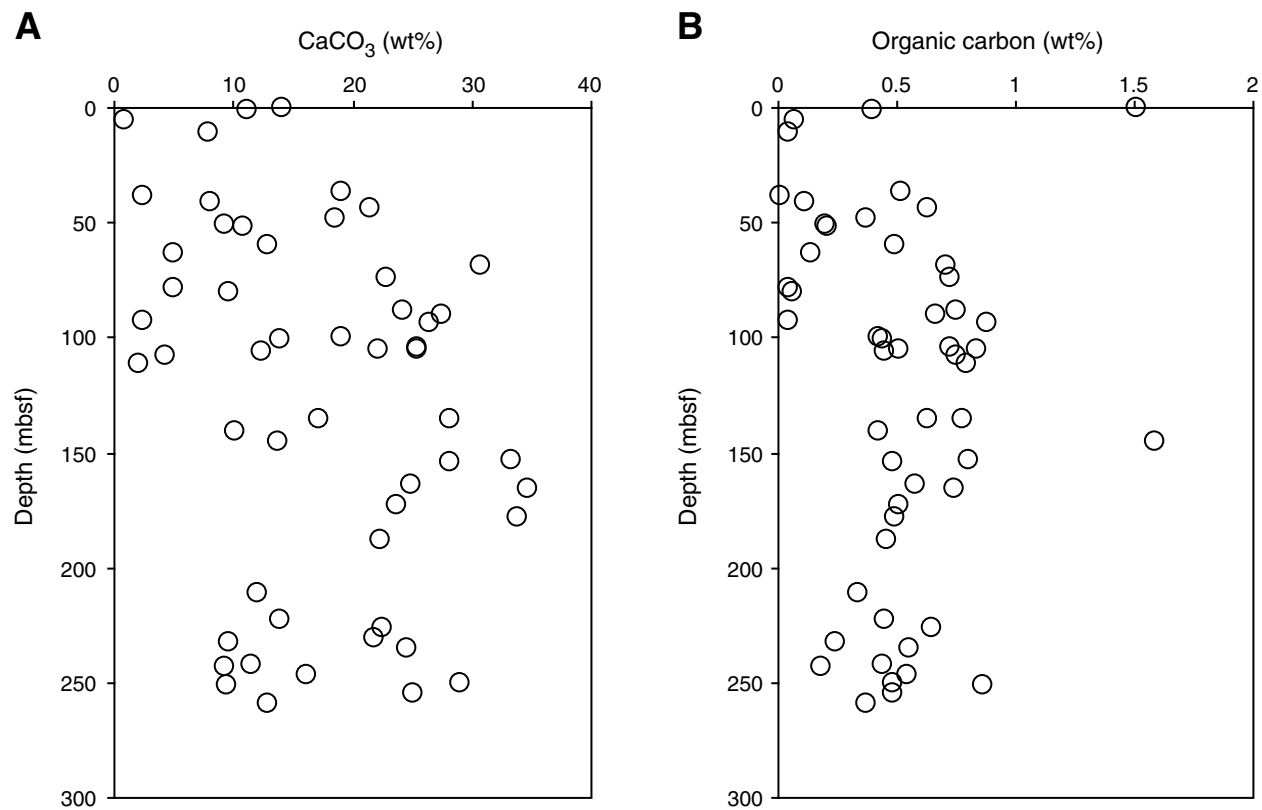
Figure F5. Solid-phase geochemical depth profiles, Site U1398. A. CaCO_3 . B. Organic carbon.



Figure F6. Pore water geochemical depth profiles, Hole U1398B. **A.** Alkalinity. **B.** NH₄⁺. **C.** Ca. **D.** Mg. **E.** Cl. **F.** ΣS.

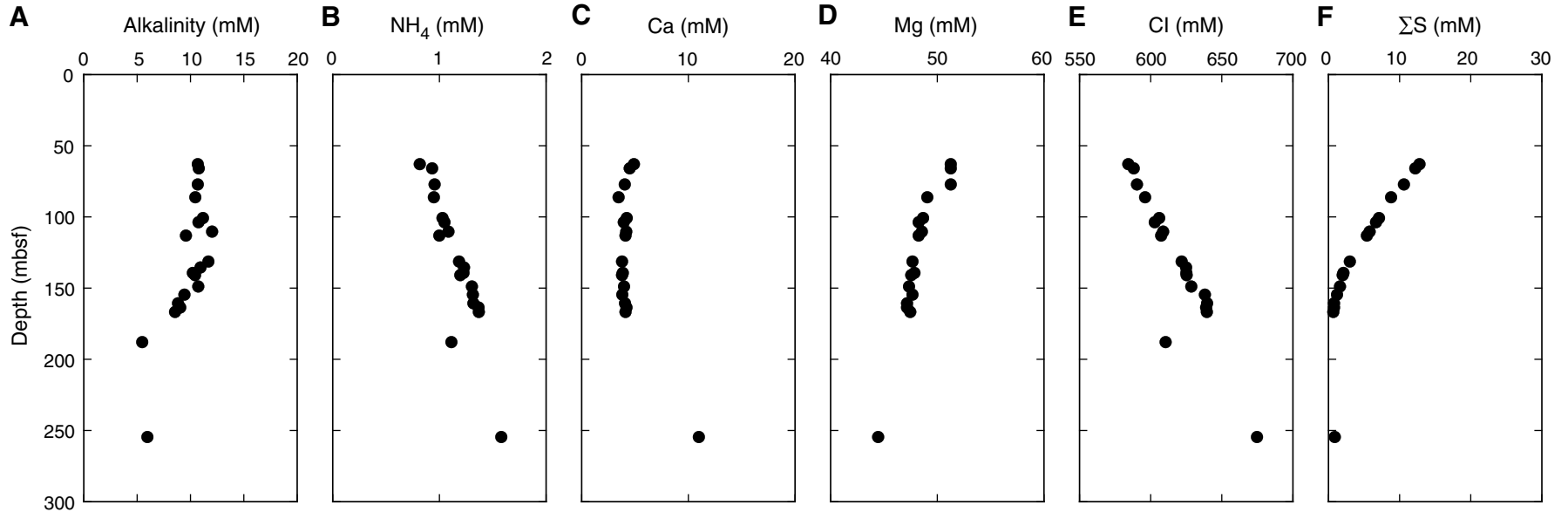




Figure F7. Magnetic susceptibility correlation, Hole U1398A (red) to Hole U1398B (blue). Magnetic susceptibility was measured on the Whole-Round Multisensor Logger (WRMSL). Negative values in the last column indicate a downhole shift. A. 0–50 mbsf. (Continued on next page.)

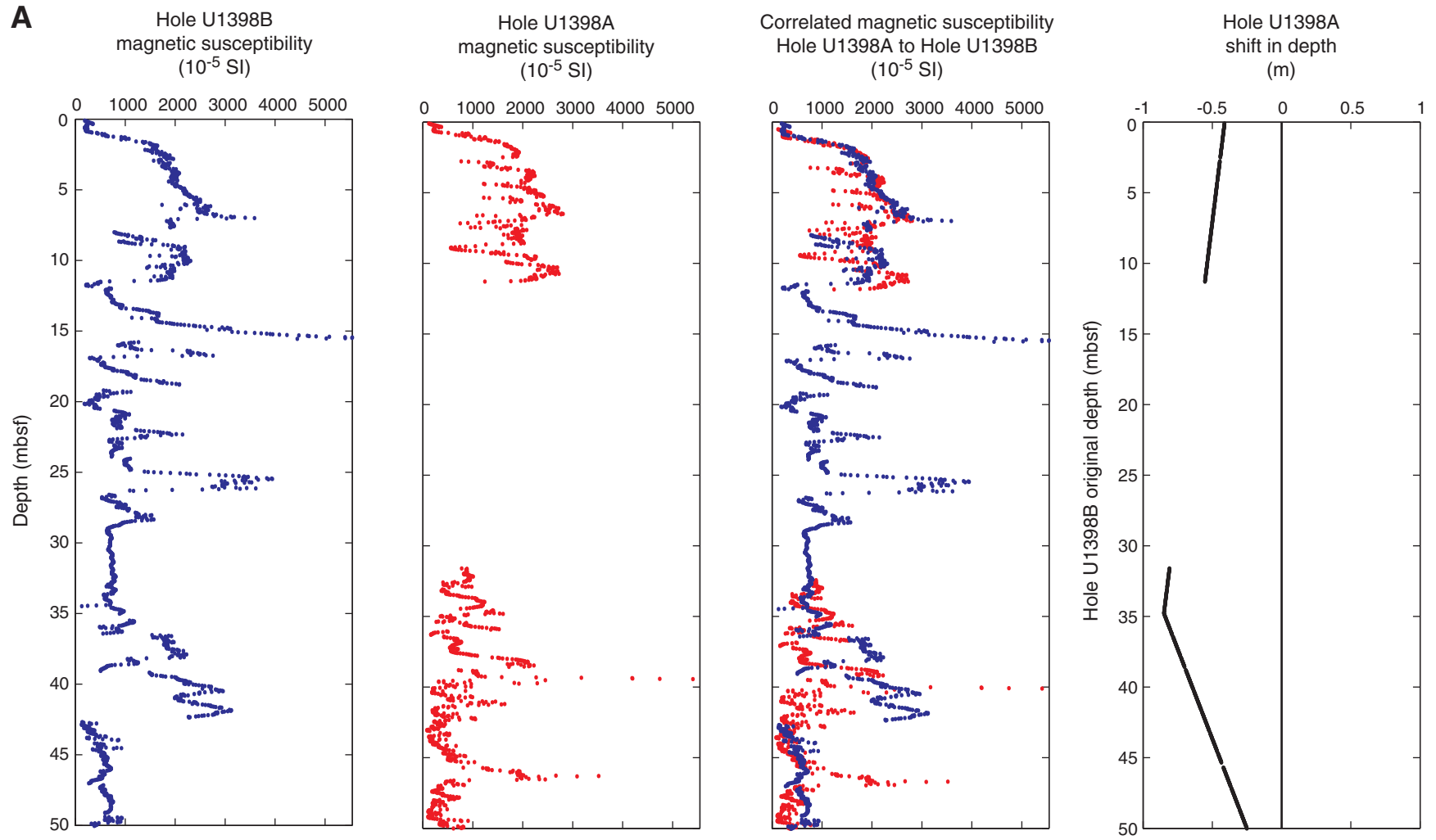




Figure F7 (continued). B. 50–110 mbsf.

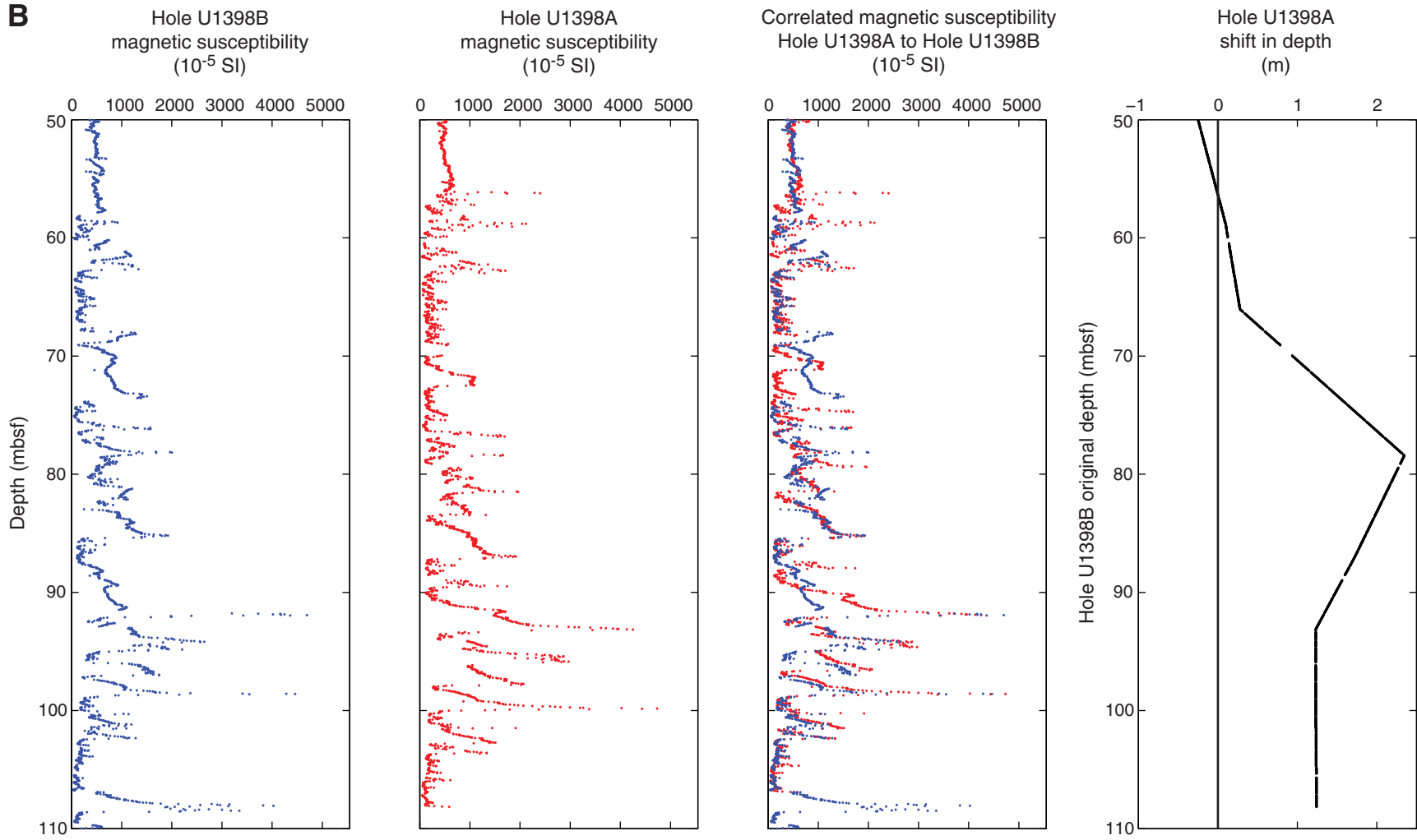




Figure F8. Physical properties, Holes U1398A (red) and U1398B (blue). AVS = automated vane shear. Small points indicate measurements on whole cores using the Whole-Round Multisensor Logger (WRMSL) or Natural Gamma Radiation Logger (NGRL). Larger circles indicate spot measurements obtained from samples of the split working half of the core.

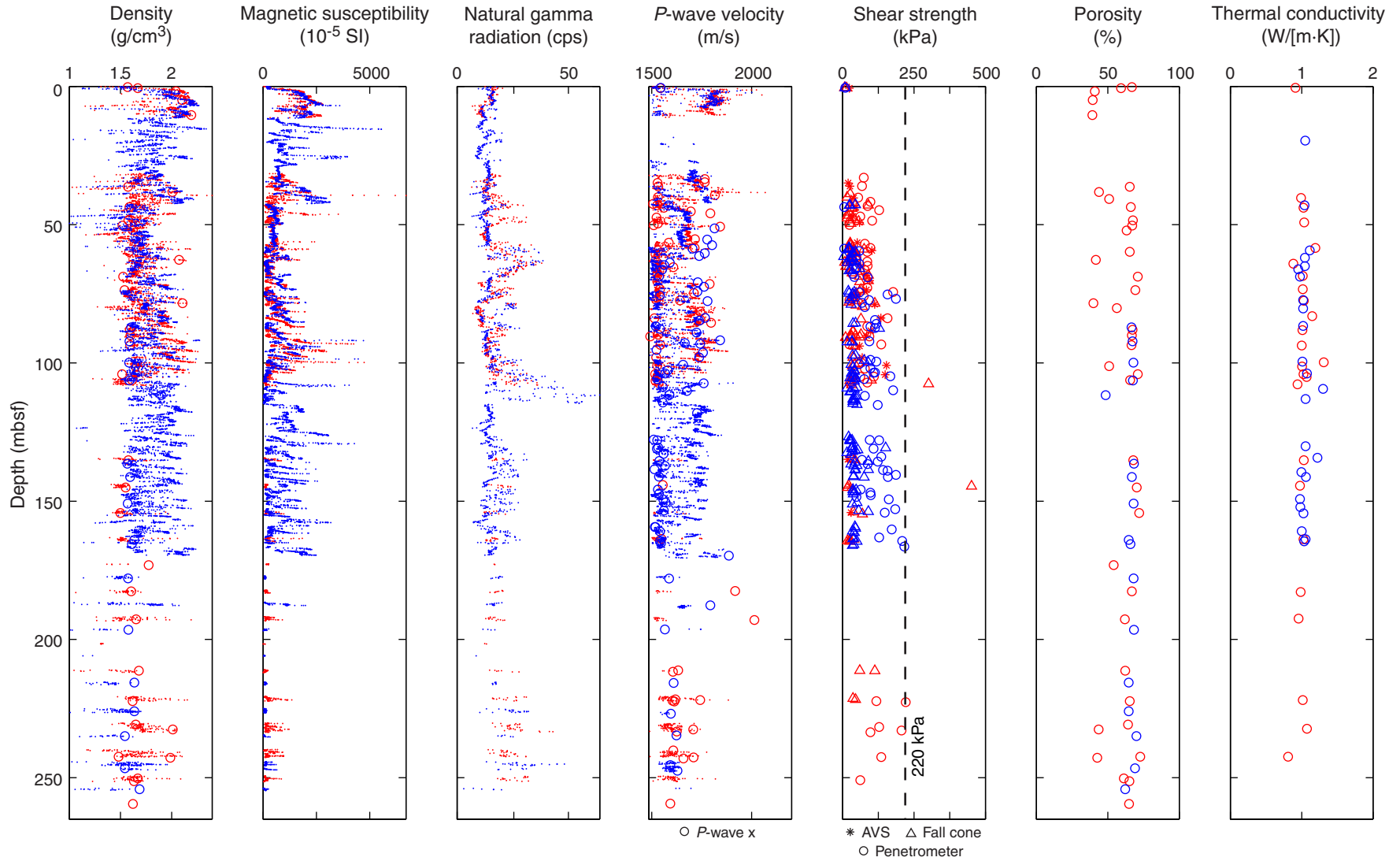


Figure F9. Temperature as a function of depth, Holes U1398A (red) and U1398B (blue). Straight line is a best fit to the measurements.

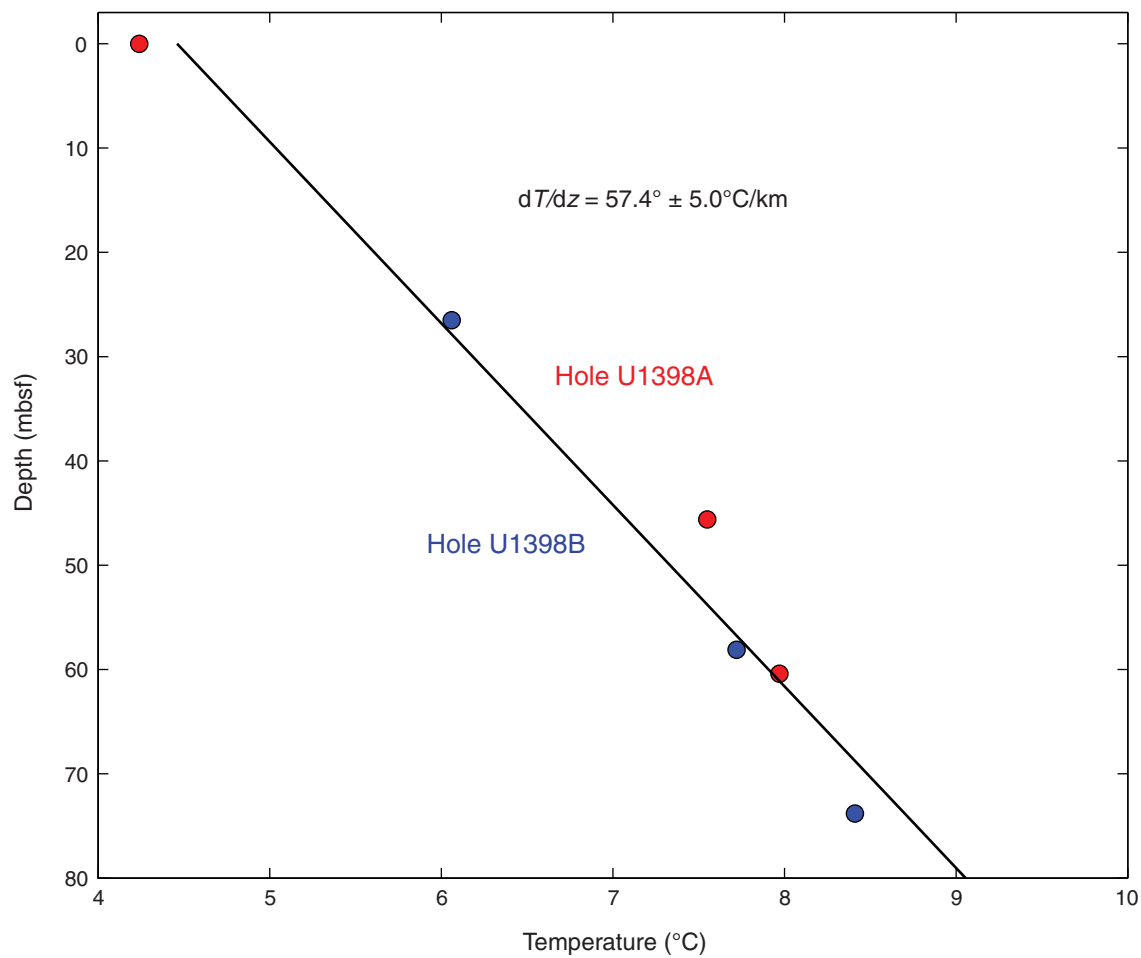


Figure F10. Plots of intensity of NRM₀ (red) and NRM₂₀ (blue) and inclination and declination after 20 mT demagnetization, Hole U1398A. For inclination data, gray points are all measurements made and red data are measurements made on hemipelagic sediment. For declination data, gray points are unoriented declinations and red points are FlexIt tool–corrected data on hemipelagic sediment. Orange points are SRM and discrete inclination guided data on hemipelagic sediment. Black squares are discrete declination and inclination measurements shown against a geocentric axial dipole (GAD) inclination of 27.0°.

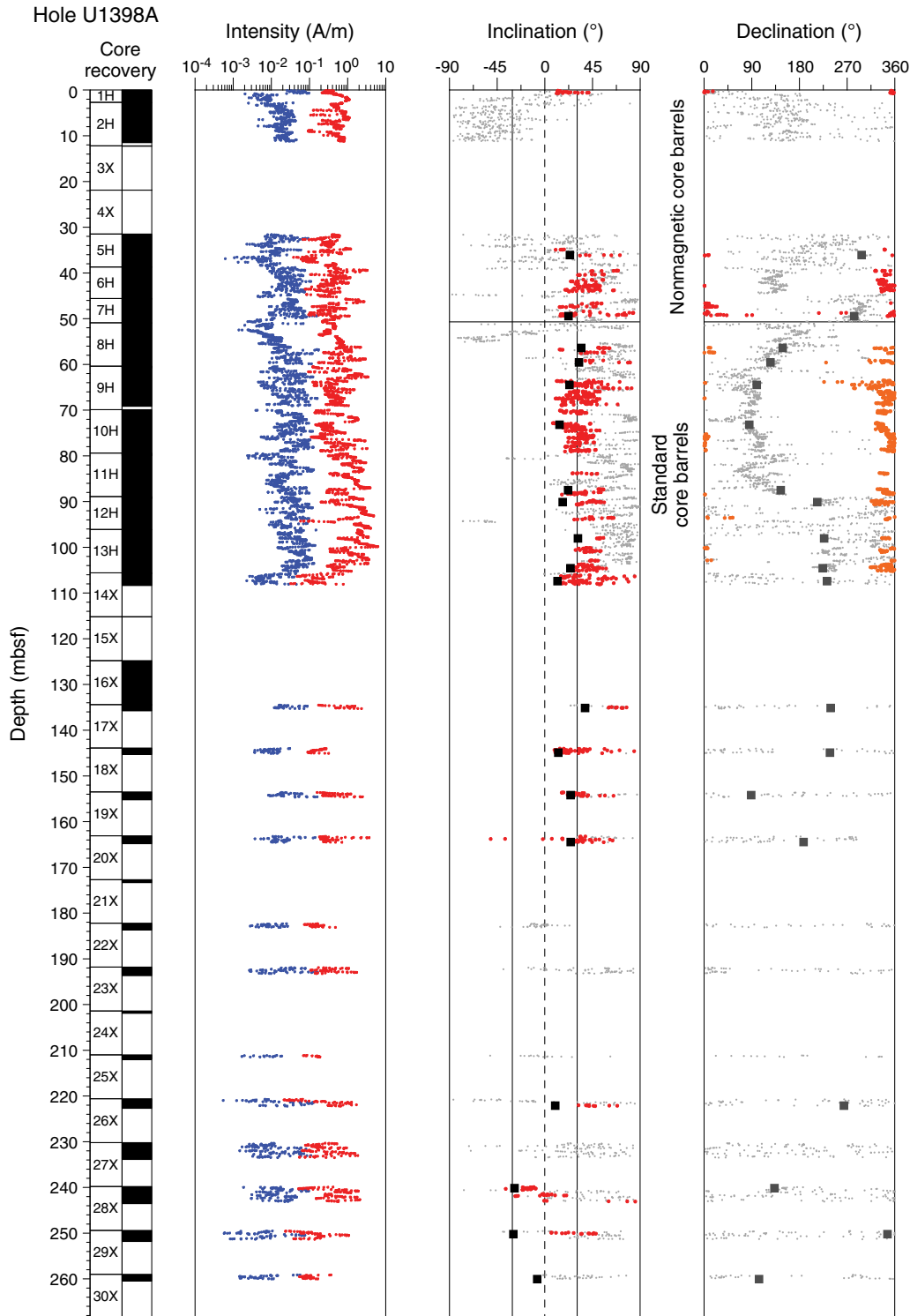


Figure F11. Plots of intensity of NRM_0 (red) and NRM_{20} (blue) and inclination and declination after 20 mT demagnetization, Hole U1398B. For inclination data, gray points are all measurements made and red data are measurements made on hemipelagic sediment. For declination data, gray points are unoriented declinations and red points are FlexIt tool–corrected data on hemipelagic sediment. Orange points are SRM and discrete inclination guided data on hemipelagic sediment. Black squares are discrete declination and inclination measurements shown against a geocentric axial dipole (GAD) inclination of 27.0° .

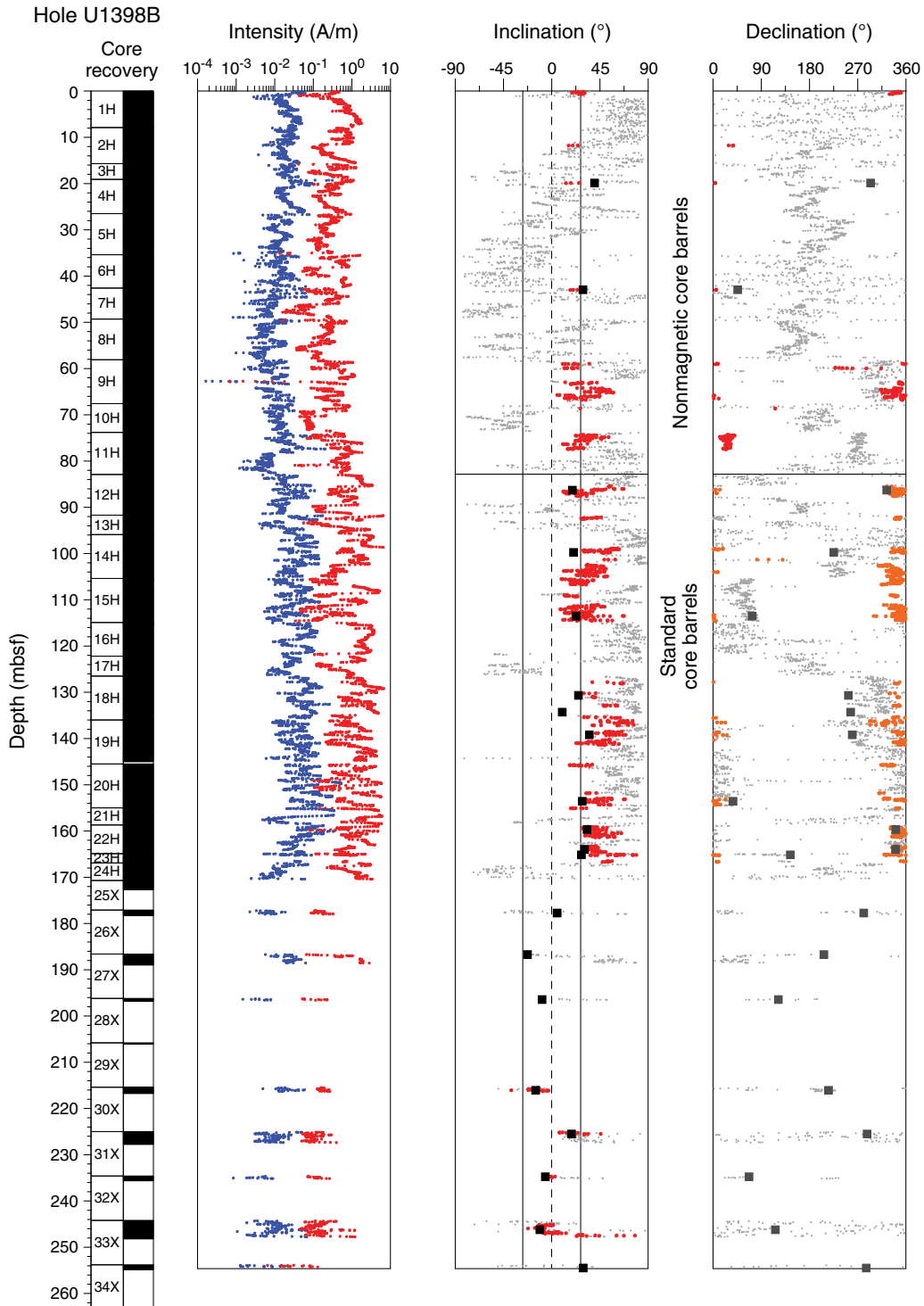


Figure F12. Zijdeveld plots, normalized NRM demagnetization curves, and normalized IRM acquisition curves for three discrete samples from Hole U1398B. NRM was demagnetized as high as 100 mT, and then IRM was imparted as high as 1000 mT. AF = alternating field.

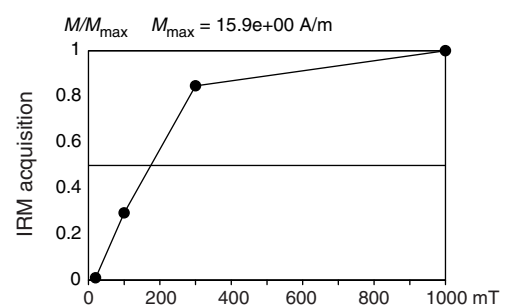
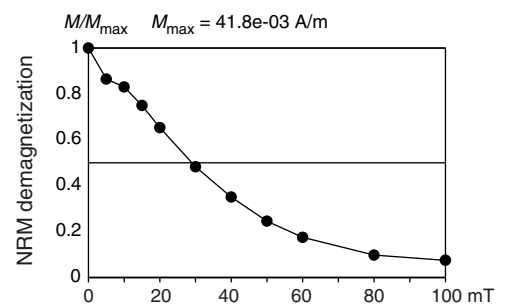
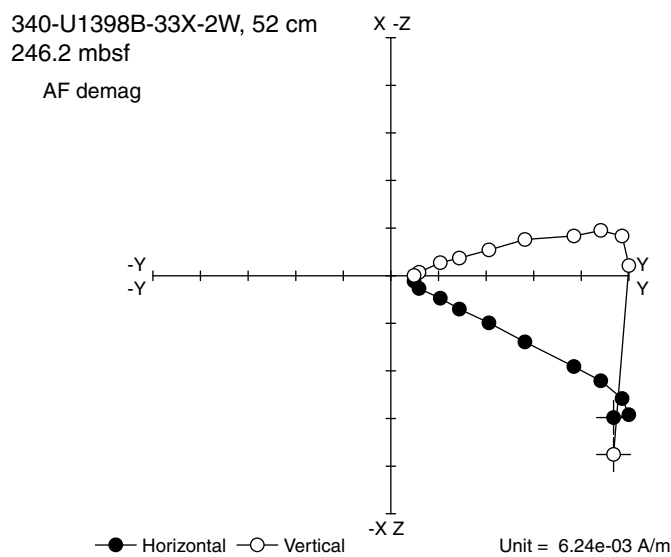
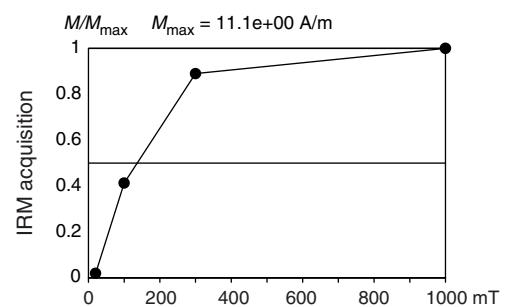
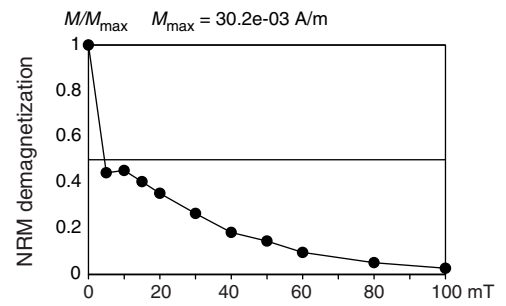
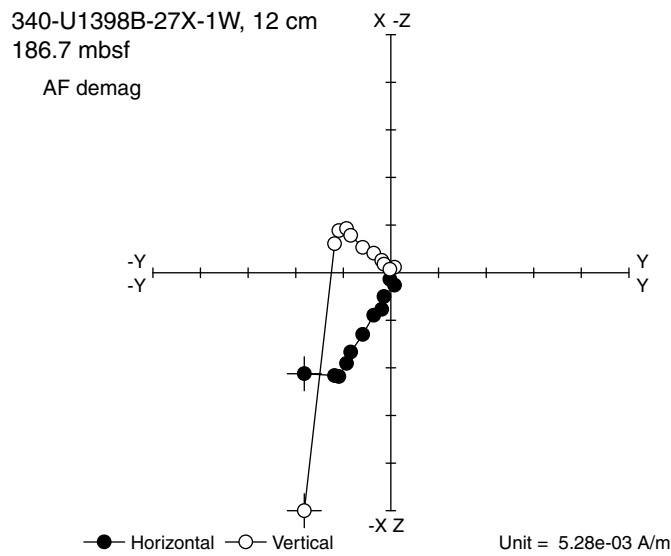
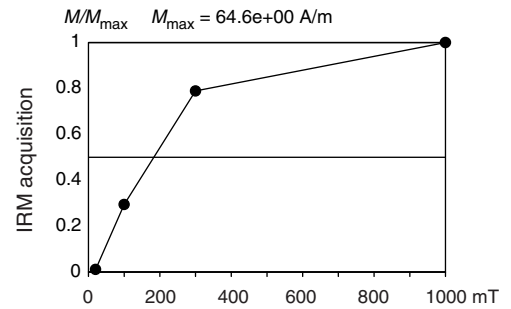
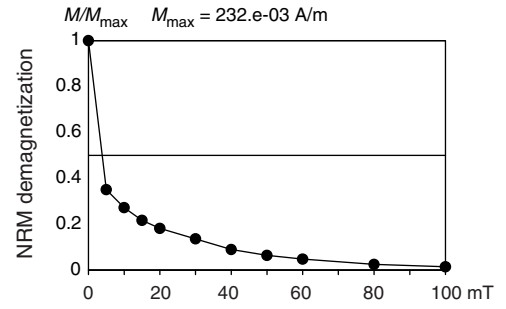
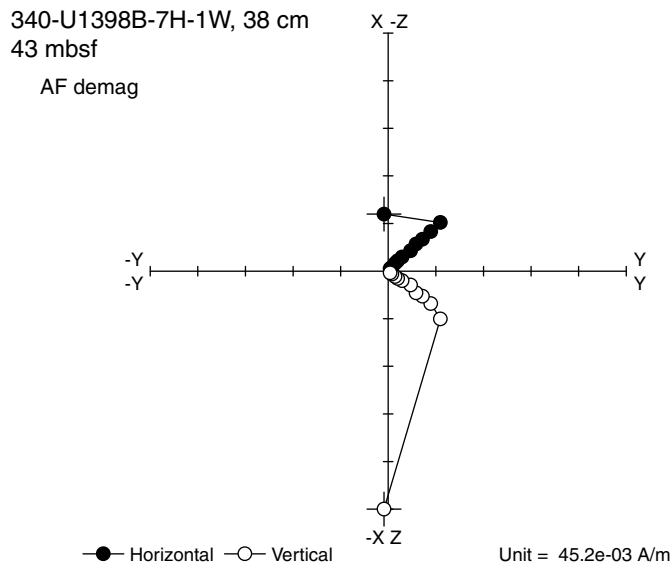


Table T1. Coring summary, Site U1398. (Continued on next page.)

Hole:	U1398A								
Latitude:	14°16.6984'N								
Longitude:	61°53.3422'W								
Water depth (m):	2935.3								
Date started (UTC*):	0300 h 24 March 2012								
Date finished (UTC*):	0145 h 26 March 2012								
Time on hole (days):	1.9								
Seafloor depth DRF (m):	2946.8								
Penetration DSF (m):	268.6								
Cored interval (m):	268.6								
Recovered length (m):	115.09								
Recovery (%):	43								
Total cores (no.):	30								
Hole:	U1398B								
Latitude:	14°16.6987'N								
Longitude:	61°53.3309'W								
Water depth (m):	2935.1								
Date started (UTC*):	0145 h 26 March 2012								
Date finished (UTC*):	1030 h 28 March 2012								
Time on hole (days):	2.4								
Seafloor depth DRF (m):	2946.6								
Penetration DSF (m):	263.4								
Cored interval (m):	263.4								
Recovered length (m):	186.75								
Recovery (%):	71								
Total cores (no.):	34								
Core	Top depth drilled DSF (m)	Bottom depth drilled DSF (m)	Advanced (m)	Recovered length (m)	Curated length (m)	Top depth cored CSF (m)	Bottom depth recovered CSF (m)	Recovery (%)	Time on deck (UTC*)
340-U1398A-									
1H	0.0	2.7	2.7	2.76	2.76	0.0	2.76	102	3/24/12 20:05
2H	2.7	12.2	9.5	8.81	8.81	2.7	11.51	93	3/24/12 21:10
3X	12.2	21.9	9.7	0.07	0.10	12.2	12.30	1	3/24/12 23:50
4X	21.9	31.5	9.6	0.00	0.00	21.9	21.90	0	3/25/12 00:50
5H	31.5	38.7	7.2	7.26	7.26	31.5	38.76	101	3/25/12 01:50
6H	38.7	45.6	6.9	7.05	7.05	38.7	45.75	102	3/25/12 03:10
7H	45.6	50.9	5.3	5.37	5.37	45.6	50.97	101	3/25/12 04:30
8H	50.9	60.4	9.5	9.91	9.91	50.9	60.81	104	3/25/12 05:50
9H	60.4	69.9	9.5	8.78	8.78	60.4	69.18	92	3/25/12 06:45
10H	69.9	79.4	9.5	10.09	10.09	69.9	79.99	106	3/25/12 08:05
11H	79.4	88.9	9.5	9.97	9.97	79.4	89.37	105	3/25/12 09:10
12H	88.9	96.1	7.2	7.29	7.29	88.9	96.19	101	3/25/12 10:00
13H	96.1	105.6	9.5	9.69	9.69	96.1	105.79	102	3/25/12 12:00
14X	105.6	115.2	9.6	2.77	2.77	105.6	108.37	29	3/25/12 13:30
15X	115.2	124.8	9.6	0.01	0.01	115.2	115.21	0	3/25/12 14:15
16X	124.8	134.4	9.6	9.68	9.68	124.8	134.48	101	3/25/12 15:45
17X	134.4	143.9	9.5	1.38	1.38	134.4	135.78	15	3/25/12 16:40
18X	143.9	153.5	9.6	1.44	1.44	143.9	145.34	15	3/25/12 17:30
19X	153.5	163.1	9.6	1.73	1.73	153.5	155.23	18	3/25/12 18:15
20X	163.1	172.7	9.6	1.72	1.72	163.1	164.82	18	3/25/12 19:00
21X	172.7	182.2	9.5	0.65	0.65	172.7	173.35	7	3/25/12 19:55
22X	182.2	191.8	9.6	1.50	1.50	182.2	183.70	16	3/25/12 21:10
23X	191.8	201.4	9.6	1.88	1.88	191.8	193.68	20	3/25/12 22:25
24X	201.4	211.0	9.6	0.52	0.52	201.4	201.92	5	3/25/12 23:35
25X	211.0	220.6	9.6	1.00	1.00	211.0	212.00	10	3/26/12 00:55
26X	220.6	230.2	9.6	2.10	2.10	220.6	222.70	22	3/26/12 02:10
27X	230.2	239.8	9.6	3.69	3.69	230.2	233.89	38	3/26/12 03:30
28X	239.8	249.4	9.6	3.75	3.75	239.8	243.55	39	3/26/12 05:00
29X	249.4	259.0	9.6	2.43	2.43	249.4	251.83	25	3/26/12 06:30
30X	259.0	268.6	9.6	1.47	1.47	259.0	260.47	15	3/26/12 08:05
340-U1398B-									
1H	0.0	7.9	7.9	7.99	7.99	0.0	7.99	101	3/26/12 11:40
2H	7.9	15.7	7.8	7.89	7.89	7.9	15.79	101	3/26/12 12:50
3H	15.7	19.1	3.4	3.47	3.47	15.7	19.17	102	3/26/12 13:55
4H	19.1	26.5	7.4	7.43	7.43	19.1	26.53	100	3/27/12 15:25
5H	26.5	35.4	8.9	8.73	8.73	26.5	35.23	98	3/27/12 16:10
6H	35.4	42.6	7.2	7.24	7.24	35.4	42.64	101	3/27/12 17:10
7H	42.6	49.3	6.7	6.77	6.77	42.6	49.37	101	3/27/12 18:20
8H	49.3	58.1	8.8	8.85	8.85	49.3	58.15	101	3/27/12 19:30

Table T1 (continued).

Core	Top depth drilled DSF (m)	Bottom depth drilled DSF (m)	Advanced (m)	Recovered length (m)	Curated length (m)	Top depth cored CSF (m)	Bottom depth recovered CSF (m)	Recovery (%)	Time on deck (UTC*)
9H	58.1	67.6	9.5	9.41	9.41	58.1	67.51	99	3/27/12 20:40
10H	67.6	73.8	6.2	6.25	6.25	67.6	73.85	101	3/27/12 22:45
11H	73.8	82.9	9.1	9.10	9.10	73.8	82.90	100	3/27/12 00:25
12H	82.9	91.7	8.8	8.83	8.83	82.9	91.73	100	3/27/12 01:15
13H	91.7	95.9	4.2	4.28	4.28	91.7	95.98	102	3/27/12 02:10
14H	95.9	105.4	9.5	9.88	9.88	95.9	105.78	104	3/27/12 03:10
15H	105.4	114.9	9.5	10.06	10.06	105.4	115.46	106	3/27/12 03:45
16H	114.9	122.2	7.3	7.39	7.39	114.9	122.29	101	3/27/12 04:30
17H	122.2	126.5	4.3	4.32	4.32	122.2	126.52	100	3/27/12 05:20
18H	126.5	136.0	9.5	9.74	9.74	126.5	136.24	103	3/27/12 06:15
19H	136.0	145.5	9.5	9.02	9.02	136.0	145.02	95	3/27/12 07:15
20H	145.5	155.0	9.5	9.63	9.63	145.5	155.13	101	3/27/12 08:05
21H	155.0	158.7	3.7	3.71	3.71	155.0	158.71	100	3/27/12 08:50
22H	158.7	164.9	6.2	6.25	6.25	158.7	164.95	101	3/27/12 09:40
23H	164.9	166.9	2.0	2.00	2.00	164.9	166.90	100	3/27/12 10:40
24H	166.9	170.7	3.8	3.87	3.87	166.9	170.77	102	3/27/12 11:35
25X	170.7	177.1	6.4	2.00	2.00	170.7	172.70	31	3/27/12 12:55
26X	177.1	186.6	9.5	1.17	1.17	177.1	178.27	12	3/27/12 13:40
27X	186.6	196.2	9.6	2.39	2.39	186.6	188.99	25	3/27/12 15:05
28X	196.2	205.8	9.6	0.58	0.58	196.2	196.78	6	3/27/12 16:20
29X	205.8	215.4	9.6	0.23	0.23	205.8	206.03	2	3/27/12 17:35
30X	215.4	225.0	9.6	1.37	1.37	215.4	216.77	14	3/27/12 18:50
31X	225.0	234.6	9.6	2.78	2.78	225.0	227.78	29	3/27/12 20:30
32X	234.6	244.2	9.6	1.03	1.03	234.6	235.63	11	3/27/12 22:10
33X	244.2	253.8	9.6	4.01	4.01	244.2	248.21	42	3/28/12 00:15
34X	253.8	263.4	9.6	1.08	1.08	253.8	254.88	11	3/28/12 01:50
Totals:			532.0	301.84	313.55				

* = ship local time was Universal Time Coordinated (UTC) – 4 h. DRF = drilling depth below rig floor, DSF = drilling depth below seafloor, CSF = core depth below seafloor. H = advanced piston corer, X = extended core barrel.

Table T2. Solid-phase geochemistry, Site U1398.

Core, section	Depth (mbsf)		Carbon (wt%)				Nitrogen (wt%)
	Top	Bottom	CaCO ₃	Inorganic	Total	Organic	
340-U1398A-							
1H-1	0.27	0.28	14.14	1.70	3.21	1.51	BD
1H-1	0.68	0.69	11.11	1.33	1.73	0.40	BD
2H-2	4.95	4.96	0.91	0.11	0.18	0.07	BD
2H-6	10.34	10.35	7.92	0.95	0.99	0.04	BD
5H-4	36.24	36.25	19.05	2.28	2.80	0.52	0.02
5H-6	38.15	38.16	2.38	0.29	0.30	0.01	BD
6H-2	40.74	40.75	8.06	0.97	1.08	0.11	BD
6H-4	43.65	43.66	21.47	2.57	3.20	0.63	0.03
7H-2	48.46	48.47	18.56	2.23	2.60	0.37	0.02
7H-4	50.37	50.38	9.22	1.11	1.31	0.20	BD
8H-1	52.075	52.085	10.76	1.29	1.50	0.21	BD
8H-7	60.14	60.15	12.81	1.54	2.03	0.49	BD
9H-2	62.75	62.76	5.04	0.60	0.74	0.14	BD
9H-6	68.70	68.71	30.72	3.68	4.39	0.71	0.03
10H-3	73.88	73.89	22.89	2.74	3.46	0.72	0.04
10H-7	78.92	78.93	5.01	0.60	0.64	0.04	BD
11H-1	80.14	80.15	9.54	1.14	1.20	0.06	BD
11H-7	88.44	88.45	24.14	2.89	3.64	0.75	0.05
12H-1	90.06	90.07	27.51	3.30	3.96	0.66	0.04
12H-3	92.87	92.88	2.41	0.29	0.33	0.04	BD
12H-4	93.66	93.67	26.41	3.17	4.05	0.88	0.04
13H-3	100.20	100.21	18.97	2.27	2.69	0.42	0.04
13H-4	100.88	100.89	13.94	1.67	2.11	0.44	0.05
13H-6	104.26	104.27	25.45	3.05	3.77	0.72	0.06
13H-7	105.08	105.09	22.13	2.65	3.16	0.51	0.05
14X-1	106.32	106.33	12.32	1.48	1.93	0.45	0.06
14X-2	107.94	107.95	4.25	0.51	1.26	0.75	0.08
17X-1	135.09	135.10	28.10	3.37	4.00	0.63	0.04
18X-1	144.97	144.98	13.80	1.66	3.24	1.59	0.05
19X-1	154.26	154.27	28.16	3.38	3.86	0.48	0.03
21X-CC	173.07	173.08	23.63	2.83	3.34	0.51	0.02
25X-1	211.30	211.31	12.03	1.44	1.78	0.34	0.02
26X-CC	222.34	222.35	13.83	1.66	2.11	0.45	0.05
27X-1	230.78	230.79	21.86	2.62	2.11	*	0.06
27X-1	230.78	230.79			2.12		0.05
27X-2	232.54	232.55	9.63	1.15	1.39	0.24	0.01
28X-2	242.40	242.41	11.54	1.38	1.82	0.44	0.04
28X-3	242.73	242.74	9.30	1.12	1.29	0.18	0.01
29X-1	250.29	250.30	29.05	3.48	3.96	0.48	0.01
29X-2	251.25	251.26	9.39	1.13	1.99	0.86	0.09
30X-1	259.41	259.42	12.89	1.55	1.92	0.37	0.03
340-U1398B-							
14H-CC	105.73	105.78	25.41	3.05	3.89	0.84	0.06
15H-5	111.98	111.99	2.11	0.25	1.04	0.79	0.06
18H-7	135.84	135.85	17.13	2.05	2.83	0.78	0.05
19H-4	140.91	140.92	10.11	1.21	1.63	0.42	0.04
20H-6	153.63	153.64	33.24	3.99	4.79	0.80	0.05
22H-4	164.08	164.09	24.84	2.98	3.56	0.58	0.05
23H-1	165.60	165.61	34.62	4.15	4.89	0.74	0.05
26X-1	177.91	177.92	33.79	4.05	4.54	0.49	0.03
27X-1	187.40	187.41	22.26	2.67	3.13	0.46	0.03
31X-1	225.94	225.95	22.43	2.69	3.34	0.65	0.05
32X-1	234.95	234.96	24.61	2.95	3.50	0.55	0.04
33X-2	246.53	246.54	16.10	1.93	2.47	0.54	0.05
34X-1	254.19	254.20	25.05	3.00	3.48	0.48	0.03

* = the difference between inorganic and total carbons produces a negative organic carbon value and should be regarded as highly uncertain. BD = below detection, values reported as 0.

Table T3. Composition of interstitial pore water, Site U1398B.

Core, section	Depth (mbsf)		Alkalinity (mM)	pH	Cl (mM)	±	Salinity	NH ₄ (mM)	Na (mM)	±	Mg (mM)	±	K (mM)	±	Ca (mM)	±	ΣS (mM)	±
	Top	Bottom																
340-U1398B-																		
9H-3	62.50	62.60	10.6	7.6	583.8		37	0.81	496.8	22.2	51.2	1.5	10.0	0.4	4.82	0.14	12.7	0.0
9H-5	65.50	65.60	10.7	7.7	587.6		37	0.93	496.7	15.7	51.2	0.6	10.3	0.3	4.45	0.06	12.1	0.2
11H-2	76.70	76.80	10.6	7.6	589.9		37	0.95	491.9	1.3	51.2	0.3	9.8	0.1	3.97	0.05	10.5	0.2
12H-2	85.80	85.90	10.4	7.6	595.7		37	0.94	486.3	5.2	49.0	0.6	9.5	0.1	3.40	0.01	8.7	0.2
14H-3	100.30	100.40	11.1	8.4	605.6		37	1.02	487.8	3.5	48.6	0.5	9.5	0.1	4.16	0.06	7.0	0.2
14H-5	103.30	103.40	10.7	7.5	602.4		37	1.04	489.9	1.2	48.2	0.4	9.6	0.2	3.89	0.05	6.6	0.2
15H-3	109.79	109.89	12.0	8.5	608.3		38	1.08	494.9	1.8	48.5	0.4	9.6	0.1	4.13	0.05	5.7	0.2
15H-5	112.71	112.81	9.5	7.3	607.0		38	0.99	494.2	1.5	48.2	0.4	9.0	0.1	4.04	0.05	5.3	0.2
18H-3	130.90	131.00	11.6	7.6	621.4		38	1.18	501.2	3.3	47.6	0.4	9.4	0.3	3.72	0.05	2.9	0.3
18H-6	134.97	135.07	10.9	10.4	624.4		38	1.23										
19H-2	138.90	139.00	10.1	8.0	624.6		38	1.22	514.8	5.2	47.8	0.5	9.6	0.1	3.78	0.00	2.0	0.3
19H-3	140.40	140.50	10.4	7.7	624.7		38	1.19	506.7	2.0	47.5	0.4	9.3	0.2	3.71	0.05	1.9	0.2
20H-2	148.36	148.46	10.7	7.9	628.1		39	1.30	514.5	3.1	47.3	0.4	9.8	0.1	3.91	0.05	1.5	0.2
20H-6	154.24	154.34	9.4	8.5	637.6		38	1.31	516.8	1.9	47.6	0.3	9.5	0.2	3.74	0.05	1.1	0.2
22H-2	160.22	160.32	8.8	7.6	639.1		39	1.31	518.8	1.4	47.1	0.3	9.3	0.2	3.99	0.05	0.7	0.2
22H-4	163.15	163.25	9.0	8.4	638.5		39	1.36	521.9	2.6	47.1	0.4	9.6	0.1	4.14	0.05	0.7	0.2
23H-1	166.30	166.40	8.5	7.6	638.9		39	1.36	520.0	4.1	47.4	0.5	9.5	0.2	4.04	0.06	0.6	0.2
27X-1	187.47	187.57	5.4	7.8	610.1		38	1.11										
34X-1	254.08	254.19	5.9	7.4	674.4		40	1.57	556.4	17.9	44.4	1.1	8.0	0.2	10.92	0.32	0.8	0.2

Section 340-U1398B-27X-1 was noted to be particularly sandy during processing and may have had significant contamination during drilling. Shaded samples in gray represent average values for Na, Mg, K, Ca, and ΣS (total sulfur) from duplicate analyses from separate runs. Orange shaded ΣS values represent values at our approximate detection limit. Samples in italics represent averages from within-run duplicates.

Table T4. Correlation point picks and depth shifts, Hole U1398A.

Original depth (mbsf)	Corrected depth (mbsf)	Difference (m)
0.308	0.278	0.031
6.477	6.970	-0.493
10.418	9.224	1.195
11.055	10.531	0.524
32.132	33.323	-1.191
38.431	40.468	-2.037
39.431	41.867	-2.436
49.845	49.687	0.157
58.801	58.705	0.097
66.048	65.769	0.279
78.417	76.069	2.347
86.941	85.213	1.728
93.148	91.918	1.230
95.564	94.461	1.104
99.832	98.600	1.232
103.569	102.331	1.237

Table T5. Samples measured for paleomagnetism, Site U1398.

Core	Measured (mT)	APC core barrel
340-U1398A-		
1H	0, 10, 20	Nonmagnetic
2H	0, 20	Nonmagnetic
3X	No, core catcher	Standard
4X	No, no sample	Standard
5H	0, 20	Nonmagnetic
6H	0, 20	Nonmagnetic
7H	0, 20	Nonmagnetic
8H	0, 20	Standard
9H	0, 20	Standard
10H	0, 20	Standard
11H	0, 20	Standard
12H	0, 20	Standard
13H	0, 20	Standard
14X	0, 20	Standard
15X	No, core catcher	Standard
16X	No, no sample	Standard
17X	0, 20	Standard
18X	0, 20	Standard
19X	0, 20	Standard
20X	0, 20	Standard
21X	No, shorter than response function	Standard
22X	0, 20	Standard
23X	0, 20	Standard
24X	No, shorter than response function	Standard
25X	0, 20	Standard
26X	0, 20	Standard
27X	0, 20	Standard
28X	0, 20	Standard
29X	0, 20	Standard
30X	0, 20	Standard
340-U1398B-		
1H	0, 20	Nonmagnetic
2H	0, 20	Nonmagnetic
3H	0, 20	Nonmagnetic
4H	0, 20	Nonmagnetic
5H	0, 20	Nonmagnetic
6H	0, 20	Nonmagnetic
7H	0, 20	Nonmagnetic
8H	0, 20	Nonmagnetic
9H	0, 20	Nonmagnetic
10H	0, 20	Nonmagnetic
11H	0, 20	Nonmagnetic
12H	0, 20	Standard
13H	0, 20	Standard
14H	0, 20	Standard
15H	0, 20	Standard
16H	0, 20	Standard
17H	0, 20	Standard
18H	0, 20	Standard
19H	0, 20	Standard
20H	0, 20	Standard
21H	0, 20	Standard
22H	0, 20	Standard
23H	0, 20	Standard
24H	0, 20	Standard
25X	No, no sample	Standard
26X	0, 20	Standard
27X	0, 20	Standard
28X	0, 20	Standard
29X	No, shorter than response function	Standard
30X	0, 20	Standard
31X	0, 20	Standard
32X	0, 20	Standard
33X	0, 20	Standard

APC = advanced piston corer.